Realistic Option Pricing Approach: Extension of the Base Model for American Option Valuation

Department of Economics and Finance

Master's Degree in Finance

Chair of Empirical Finance

Supervisor:

Prof. Giacomo Morelli

Co-supervisor:

Prof. Paolo Santucci de Magistris

Candidate:

Domenico Mancini

ID: 746481

Academic Year 2022/2023

Abstract

This thesis follows Zumbach's years of work in achieving a realistic option pricing framework. Our contribution is implementing a method to price American options that were not included in the original model. By replicating, verifying, and extending the base model, we have developed a consistent and robust environment for price and analyze options.

The first chapter introduces the background of option pricing, exploring the history and the significant innovations. Section 1.1 is dedicated to explaining the foundational Black and Scholes (1973), Merton (1976) model, highlighting the problems, and showing how the practitioners have tried to overcome them. We conclude this section by explaining the framework and method of the Zumbach and Fernández (2013) model, the leading paper we track in this thesis. In the second half of this chapter, Section 1.2, we examine the major financial *stylized facts* included in the Zumbach realistic model.

The second chapter illustrates the methodology used, moving through the crucial steps needed to obtain the option pricing. The methodology replicates the work of Zumbach, extending it at the end of the chapter. The American option pricing extension is performed with the Least Square Montecarlo by Longstaff and Schwartz (2001). Merging the two models allows us to augment both methods and obtain a realistic pricing approach to price American and European options.

The last chapter analyzes the thesis results, showing the difference between European and American options. The comparison is made at different levels: price, smile, smirk, and term structure. Considering different time frames with unique market conditions, we can extrapolate the market expectations from the option characteristics.

Keywords: *Option Pricing, American Options, ARCH, Monte Carlo, Volatility Forecast, Implied Volatility, Heteroscedasticity, Leverage effect, Equivalent Martingale Measure, Risk Premium.*

Contents

Introduction **1**

1 Background **3**

1.1 Option pricing framework . . . 3

1.1.1 Black, Scholes and Merton Model . . . 3

1.1.2 BSM Model Limitations . . . 5

1.1.3 Beyond Black and Scholes . . . 6

1.1.4 The Zumbach and Fernández (2013) Framework . . . 8

1.1.5 American options . . . 9

1.1.6 The Least Square Montecarlo . . . 11

1.2 Stylized facts and empirical findings . . . 13

1.2.1 Heteroscedasticity . . . 13

1.2.2 Leverage effect . . . 15

1.2.3 Time reversal Invariance . . . 16

1.2.4 Returns Distribution . . . 16

2 Methodology **19**

2.1 Returns . . . 19

2.1.1 Returns aggregation . . . 20

2.2 Volatility Estimation . . . 21

2.2.1 GARCH(1,1) . . . 21

2.2.2 Long Memory ARCH . . . 22

2.2.3 Parameters estimation . . . 23

2.2.4 Volatility Forecast . . . 24

2.3 Model Drift . . . 26

2.4 From Physical to Risk-Neutral probability measure . . . 26

2.4.1 Equivalent Martingale Measure (EMM) . . . 27

2.5 Small δt expansion . . . 29

2.6 Monte-Carlo Simulation . . . 32

2.7 Option Pricing . . . 32

2.7.1 No Arbitrage Principle . . . 33

2.7.2 Monte Carlo pricing scheme . . . 34

2.8 American Option pricing . . . 35

3 Applied Model **38**

3.0.1 Model Set-Up . . . 38

3.0.2 Option Pricing results . . . 43

3.0.3 Implied Volatility . . . 46

Conclusions **49**

A Figures **51**

List of Figures

1 *Volatility surface for SP500 (left) and EUR/USD (right). Source: Bloomberg* 5

2 *Daily logarithmic returns for the SP500 and Eur/Usd time series and their autocorrelogram. Data source: Bloomberg* 13

3 *Daily Squared logarithmic returns for the SP500 and Eur/Usd time series and their autocorrelogram. Data source: Bloomberg* 14

4 *SP500 and Eur/Usd residuals after applying ARCH(3) model. Correlograms of the squared returns after applying ARCH(3).* 15

5 *News impact curves for the SP500. Where h(t) is the volatility* 16

6 *Skewness and relative excess Kurtosis at increasing time intervals for SP500.* 17

7 *Effective variance calculated with the leveraged multiscale ARCH, plotted with the returns at different scale.* 39

8 *The final prices S_n from the Monte Carlo compared with the two approximations $F_n \exp(R)$, and $F_n\Big(1 + R + \frac{R^2}{2} + \sum_i(\mu_i - r_{rf}) - \frac{y}{2} - \frac{\sigma_{int}^2}{2}\Big)$* 41

9 *Top figure: 1 year forecast estimation. Bottom figure: 6 months rolling estimation, used to calculate μ.* 41

10 *Market price of risk λ and risk premium ϕ* 42

11 *The different probability density functions for the final prices S_n in $\mathbb{P}$ and $\mathbb{Q}$ measures. Plotted at increasing $\sigma_\infty = 0.1, 0.2, 0.4$. Two different time horizons: 30 days and 260 days.* 43

12 *American and European put option prices compared. Maturity 30 days* . . 44

13 *American and European put options price surfaces. Maturity 1 year* 45

14 *Standard error boxplots for increasing time to maturity: n=30,90,150,210,270 (days). N=40000 (simulations)* 46

15 *Implied volatility surface for January 2004 American put options* 47

16 *Implied volatility surface for October 2008 American put options* 47

17 *Volatility smile for January 2004 American put options. Calculated at different time horizons.* 47

18 *Term structure for January 2004 American put options* 48

19 *Term structure for October 2008 American put options* 48

20 *Comparison between the two risk aversion functions e^{-x} and $\frac{1}{1+e^x}$.* 51

21 *SP500 historical prices from '02-Jan-1996' to '28-May-2010'. Data source: Bloomberg.* 51

22 *Relative returns for SP500 at different time horizons τ* 52

23 *Laguerre polynomial of order 1 through 5* 52

24 *Chebyshev polynomial of order 1 through 5* 53

25 *Impact of the leverage effect λ_{lev} on the simulation, from high left (lower) to bottom right (highest). The number of trajectories $N = 2000$ and the time steps $n = 90$.* 53

26 *The distributions and the cross-plot between the final prices S_n elements: S_n, R and σ_{int}.* 54
27 *The drift μ, the dividend yield q, and the risk-free r_{rf} compared. $\beta = 0.075$ and $\sigma_{rp} = 0.12$* 54
28 *Price surfaces for European call options, European put options, and American put options. Maturity 1 year* 55
29 *Close-up between the American and European price surfaces. Maturity 1 year* 55
30 *European and American option prices at increasing maturities.* 56

Introduction

In the financial derivatives framework, particularly within option pricing, a crucial challenge is capturing the actual behavior of the financial assets. The traditional models often can not replicate the recent markets' evidence and anomalies, and a realistic underlying process is an essential feature of any option pricing model that aims to capture such empirical findings. This thesis follows the work of Zumbach (2002, 2006, 2009, 2012, 2013), spanning over a decade, in which the author created a quantitative practical framework valuable in different contexts. Our work aims to replicate, verify, and extend the model and method established by Zumbach. The central theme of his approach is to incorporate the underlying process with the significant financial *Stylized facts*. This way, we can realistically simulate and reproduce the financial assets' behaviors. In addition to that, American options present a layer of complexity that demands models with a critical sense of realism. The original work did not present a way to estimate such derivate prices, leaving this challenge open. The thesis contribution will be, in fact, a base model extension that can consistently and robustly estimate American options prices under the Zumbach framework.

The Zumbach option pricing framework we will expose in the thesis follows the route started by Rubinstein (1976) and Brennan (1979), followed by Duan (1995), Heston and Nandi (2000), Chorro et al. (2008) and augmented by Christoffersen et al. (2010). The methodology to pursue option pricing is fractioned into many steps, most of which were assembled by Zumbach and Fernández (2013), the leading paper followed in this paper. We will start by calculating relative returns instead of logarithmic ones accordingly with O'Neil and Zumbach (2009). Relative returns are better suited for our realistic purposes and better capture the distributional properties of financial returns. At its core, the method has an ARCH volatility estimation based on the milestone work of Engle (1982). The autoregressive heteroscedastic variance, later augmented by Bollerslev (1986) with the GARCH model, is the process we will adopt to perform the underlying paths simulation. The GARCH methodology allows for flexible modification of the standard model, which can be easily augmented to capture empirical observations. The precise extension adopted in this thesis is the Long Memory ARCH by Zumbach et al. (2014), which allows for *leverage effect* and a variance estimation considered over different time horizons, offering a more accurate lens to view volatility dynamics in the market. For some specific uses, we need an ARCH forecast that will be performed following the specifications of Zumbach (2002) and Zumbach (2006). Afterward, we will explore the *Monte Carlo* simulation method used to simulate the underlying price process, and the technical aspects will observe the Jaeckel (2002) methodology. By abandoning the traditional Brownian motion in the Monte Carlo simulation, we will employ a process underpinned by a heteroscedastic variance with leverage effects and the parameters estimated to replicate the distributional features of the underlying. The simulated paths have a pronounced dispersion that offers more authentic option prices that resonate with market behaviors. Another pivotal model step is

the probability measure change from the physical $\mathbb{P}$ to the risk-neutral $\mathbb{Q}$. On the path left by Duan (1995) and Christoffersen et al. (2010), in the O'Neil and Zumbach (2009) paper, the authors presented a methodology to calculate this transition analytically using the *Radon-Nikodym* derivative $\frac{d\mathbb{Q}}{d\mathbb{P}}$. This way, the model can simulate processes in the $\mathbb{P}$ measure realistically and only after transferring them into the risk-neutral. We will conclude by extending the present framework to American Options using the pricing method by Longstaff and Schwartz (2001).

American options have early exercise features, meaning the holder can exercise the option before maturity. The buyer must pay for this additional feature, which is why American options require a different pricing approach. While exercising a call option before maturity is rarely convenient, the put option differs, specifically if the underlying price is way down with little space for further drawdowns. We will find a rule to assess the convenience of exercising the option early, trying to solve an optimal stopping problem. A simulation-based approach, such as the Zumbach one, is the classic environment in which American options are usually priced, thus making the Zumbach model's extension achievable. The American pricing approach might be time-consuming and computationally challenging, so we will apply the LSM method by Longstaff and Schwartz (2001) to overcome those problems. This method relies on an approximation of the expected future value integral, and this way, we will neither need to simulate the underlying recursively nor solve an integral at each time step. With some modifications, the possible implementation of these two models would create an efficient and time-saving method to consistently and realistically price American options.

This approach allows us to price the American and European options' specifications and compare the resulting prices. We will retrieve crucial information from the prices, implied volatility level, smile, smirk, and term structure. We will analyze the dynamics between European and American options and how the prices respond to changes in the underlying model structure. All these options' characteristics will allow us to understand the details and the drivers of the option's value and market expectations. To conclude, by comparing different market conditions, we will be able to study how the options features respond to the changes in the market, and how the market expectations influence the option prices.

1 Background

1.1 Option pricing framework

Option pricing is the process of determining the fair value of an option. This valuation is crucial for efficient capital allocation, risk management, trading, and more. Options grant holders the right, but not the obligation, to buy or sell an underlying asset at a predetermined price within a specified timeframe. The pricing challenge lies in the multifaceted nature of options; various factors influence their value, creating a non-linear relationship between the underlying and option prices. For this reason, several studies with many different approaches tried to solve the pricing puzzle. The following section will introduce the option pricing framework where our proposed model lies. The scope of this section is to understand the fundamental principle of the classic option pricing approach, underlying the problems, and explain how we tried to solve them.

1.1.1 Black, Scholes and Merton Model

The fundamental option pricing model is the Black and Scholes (1973) and Merton (1973) work (BSM). The model's success can be attributed to its ability to capture the essential factors influencing an option price, and one of the model's greatest strengths is its accessibility. The BSM formula is simple to understand and apply, especially for European-style options. As we can imagine, the model's simplicity comes with several downsides. Despite this, the model is still prevalent and very useful; for example, it makes it possible to map the volatility surface from the option prices.

The Merton (1973) approach to deriving the BSM equation is about creating a riskless portfolio Π, which is constructed by underlying and derivative positions. The portfolio Π is riskless because the underlying and the option are affected by the same source of risk, and we can choose particular positions to hedge such risk. If no arbitrage opportunities exist, Π should earn the risk-free return r. The assumptions[1] behind the model are:

- The underlying follows a Brownian Motion, and the variance rate of return σ and the drift μ are constants.
- The risk-free rate r is known and constant for all maturities. All securities share this short-term interest rate.
- Short selling is permitted.
- All security trading is continuous, with no riskless arbitrage opportunities.
- No dividends are paid during the life of the derivative.

[1] Washburn and Dik (2021)

- All securities are perfectly divisible, and there are no transaction costs.[2]

The fundamental theory behind the development of the BSM equation is Ito's Lemma, a fundamental result in stochastic calculus. It provides a way to calculate the differential (rate of change) of a function of a stochastic process. The stock price process is an Ito process $dS = \mu S dt + \sigma S dz$ where μ is the expected rate of return (drift) and the term $\sigma S dz$ represents the stochastic part (diffusion). Now, by applying Ito's Lemma on the Stock process, we can define our option (f) behavior:

$$df = \Big(\frac{\partial f}{\partial S}\mu S + \frac{\partial f}{\partial t} + \frac{1}{2}\frac{\partial^2 f}{\partial S^2}\sigma^2 S^2\Big)dt \; + \; \frac{\partial f}{\partial S}\sigma S dz \tag{1}$$

From equation 1, we see that the stochastic component underlying f and S is the same (dz). Thus, we can select a portfolio that eliminates that source of risk in order to price the option in the risk-neutral space consistently. The portfolio composition is short on the option and long Δ units of the underlying such that $\Pi = -f \; + \; \frac{\partial f}{\partial S}S$. The derivative of the option with respect to the underlying, which we called Δ, is a crucial quantity that allows us to hedge the portfolio from the Ito process risk. The change in the value of the portfolio is $\Delta\Pi = -\Delta f \; + \; \frac{\partial f}{\partial S}\Delta S$; substituting[3] S with its equation and equation 1 into $\Delta\Pi$ we obtain

$$\Delta\Pi = \Big(-\frac{\partial f}{\partial t} - \frac{1}{2}\sigma^2 S^2 \frac{\partial^2 f}{\partial S^2}\Big)\Delta t \tag{2}$$

Since equation 2 has no dz inside, the portfolio must return the risk-free rate r so that we can write $\Delta\Pi = \Delta t \Pi r$. Finally, it is possible to derive the Black and Scholes partial differential equation (PDE) by arranging all the precedent equations together.

$$rf = \frac{\partial f}{\partial t} + rS\frac{\partial f}{\partial S} + \frac{1}{2}\sigma^2 S^2 \frac{\partial^2 f}{\partial S^2}, \; = \theta + rS\Delta + \frac{1}{2}\sigma^2 S^2 \Gamma \tag{3}$$

where Δ, Γ and θ are the so called "option Greeks". The most outstanding aspect of BSM PDE is how it describes the dynamic behavior of the option's price over time. The equation simply and elegantly encapsulates the principal factors determining the derivative price. In particular, θ or $\frac{\partial f}{\partial} t$ denotes the time decay; options lose value as time passes, mainly if they are out of the money (OTM). Secondly, Δ measures the sensitivity of the option's price to changes in the underlying asset's price. Moreover, the BSM creates a clear relationship between the option price and the volatility. Higher volatility leads to more significant price fluctuations and, in turn, positively affects the option's value.

As the model assumption suggest, the pricing in the BSM model is under the risk-neutral probability space[4]. Under the risk-neutral measure $\mathbb{Q}$, the distribution of future stock prices is log-normal. From that, we can explicitly retrieve the probability distribution

[2] J. C. Hull (2012)

[3] and moving from continuous into discrete time

[4] In the next chapter, we will go deeper into this concept, especially considering the change of measure from the physical $\mathbb{P}$ into the risk-neutral $\mathbb{Q}$.

of the underlying under the risk-free measure. This fundamental concept, Risk Neutral Density(RND) $f_{t,T}$, is one of the pivotal theories in the option pricing realm. The density for S_T conditional to S_t, which we defined as Risk-neutral Density $f_{t,T}$, can be retrieved directly from the solution of the PDE[5]

$$p[S_T, T|S_t, t] = \frac{1}{\sqrt{2\pi\tau}\sigma S_T} \exp\left[-\frac{1}{2}\left(\frac{\log(S_t) - \zeta}{\sigma\sqrt{\tau}}\right)^2\right] = f_{t,T} \tag{4}$$

which is calculated in the transition period τ from t to T, and $\zeta = \log(S_t) + (\mu - \frac{1}{2}\sigma^2)\tau$.

1.1.2 BSM Model Limitations

As with any pioneering framework, the Black, Scholes, and Merton model's initial assumptions and simplifications, intended to make the model tractable, did not capture all the complexities of real-world financial markets. These limitations have the merit of paving the way for subsequent advancements in the field. Researchers recognized the challenges the Black-Scholes model's assumptions posed and developed more refined and sophisticated models. Their goal was to replicate actual market behaviors better, handle the recognized shortcomings, and provide a more exhaustive framework for option pricing.

In the Black-Scholes model, volatility σ is assumed to be constant over the option's life. However, in actual financial markets, the volatility of assets can change over time. Using the implied volatility surface derived from the market option prices, we can quickly notice the problems of the BSM pricing scheme. Since volatility is the only free parameter in the BSM equation, we can use market option prices to derive different levels of volatility and construct the surface. As we anticipated, this characteristic of the BSM model is one of the reasons why the model is still prominent.

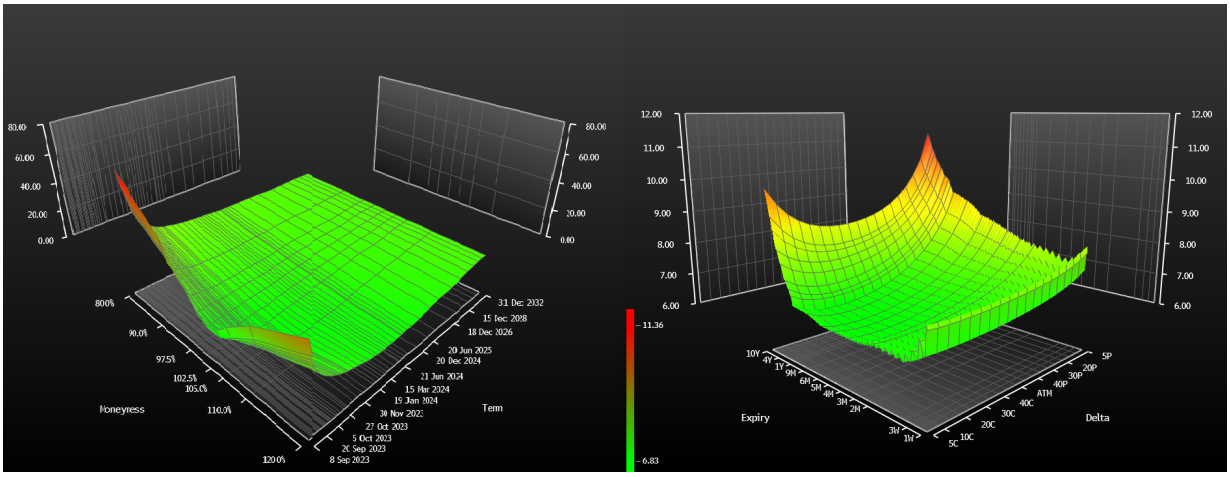

Figure 1: *Volatility surface for SP500 (left) and EUR/USD (right). Source: Bloomberg*

If the BSM is correct, the implied volatilities should not depend on the strike, observation

[5]Eric Jondeau (2010)

time, or maturity. In other words, they should appear completely flat surfaces. The Implied volatility surfaces have different components that characterize them. At the heart of the implied volatility surface is the term structure, which is the relation between the implied volatility and the maturity of the derivative. Secondly, the implied volatility of an option as a function of its strike price is known as a volatility smile. Finally, the volatility smirk refers to a pattern observed in option implied volatilities as it moves across different strike prices. More accurately, this is the pattern that emerges when far OTM (ITM) call (PUT) options show higher implied volatility compared to the ITM (OTM). According to the BSM assumption, these key factors should not affect the volatility or the option price. However, as shown in Figure 1, the market implied volatilities show changes in the overall levels, smiles, smirks, and term structure. Therefore, the actual RND inferred from market prices of options might differ from the simple log-normal distribution suggested by BSM.

The Black-Scholes model underlying asset prices are log-normally distributed; more accurately, prices follow a geometric Brownian motion. While the log-normal distribution captures that stock prices cannot go below zero, it does not capture the full range of potential price behaviors observed in real-world financial markets. For example, the actual distribution of returns often has negative skewness or "fat tails," meaning extreme price changes occur more frequently than predicted by the log-normal distribution. In general, the strict distributional assumption does not allow for incorporating realistic behaviors of the financial time series. The two limitations previously explained are crucial, but there are still some other minor deficiencies worth mentioning. For example, the Black and Scholes model's basic form only prices European options and does not directly apply to American options. Furthermore, the model assumes that markets are perfectly liquid, allowing continuous trading without impacting the stock's price, but in reality, liquidity constraints can arise. To conclude, the BSM model assumes that stock price movements are continuous, without jumps. In reality, stock prices can and do make sudden jumps.

1.1.3 Beyond Black and Scholes

As market practitioners increasingly implemented and tested the Black-Scholes model, the limitations emerged more prominently, revealing disparities between theory and empirical market realities. In this section, we will explore beyond the foundational framework of Black and Scholes, exploring the approaches that evolved after. These subsequent models, informed by both the strengths and shortcomings of their predecessors, research into alternative assumptions, dynamic adaptations, and new computational techniques, all in search of a more accurate option pricing model.

After Black, Scholes, and Merton's model, two dominant approaches emerged: structural and non-structural methods. What differentiates the two categories is the approach to recover the Risk-neutral density (RND) from observed options. We explained that in the BSM model, the underlying process follows a lognormal diffusion process with constant

volatility. Despite such assumptions, in the previous section, we showed that, in reality, these simplifications do not hold. The literature has focused on deriving the Risk-neutral density (RND) with the intention of overcoming the BSM assumptions. The crucial difference between Structural and Non-structural approaches is, for instance, in the methods used to obtain the RND[6]. On the one hand, the structural models propose a specific structure for the stock price and, usually, for the volatility. Generally, those models are controlled by a set of parameters $\theta \in \Theta$ that directly influence the estimation of the Risk-Neutral density, such as $f_{t,T} = f^{\theta}_{t,T}$. On the other hand, non-structural models do not fully describe the prices and volatility dynamics. The risk-neutral density (RND) estimation is performed separately between each t and T without a specific process for the underlying. Non-structural processes can be further divided into parametric, semiparametric, and non-parametric models. The first model (parametric) fully describes the RND, while the other two (semi-non-parametric) propose an approximation.

One of the most popular classes of Structural models is the Stochastic Volatility (SV) approach. Recognizing that the assumption of constant volatility in the BSM framework was too rigid to capture market complexities, researchers proposed models where the volatility follows a stochastic process. The model proposed by Heston (1993) has become one of the cornerstones in the family of the SV approach, where the following equations describe the stock S_t and the variance σ_t^2 process:

$$dS_t = \mu S_t dt \ + \ S_t \sqrt{\sigma_t^2} dW_{1,t} \tag{5a}$$

$$d\sigma_t^2 = k(\sigma_\infty^2 - \sigma_t^2)dt \ + \ \epsilon \sqrt{\sigma_t^2} dW_{2,t} \tag{5b}$$

The parameters of the processes are $\theta = (\sigma_\infty^2, k, \epsilon)$ and σ_∞^2 is the long-term variance or the long-run average. The two stochastic components are the Brownian Motions W_1 and W_2 correlated with a correlation coefficient ρ. The variance σ_t^2 follows a mean reverting square root process (Cox-Ingersoll-Ross process), and the stock S_t dynamics is a geometric Brownian motion. The Heston model's capability to produce a closed-form solution for European option prices makes it particularly attractive. Moreover, the Heston model can efficiently capture two fundamental stylized facts: the heteroscedastic and the mean-reverting behavior of the volatility. The first is moved by a stochastic factor in its parametrization (vol-of-vol ϵ), and the second is controlled by $k(\sigma_\infty^2 - \sigma_t^2)dt$. There are several other stochastic volatility models worth mentioning like J. Hull and White (1987), Stein and Stein (1991) and Carr and Sun (2007); each of these models gave a substantial contribution to the SV option pricing approach. In the Structural family, other methods were developed to obtain a consistent pricing model. One of them is the models with jumps; a prominent example is the Merton (1973) Jump Diffusion model. In this framework, the asset price follows a standard geometric Brownian motion with Gaussian jumps.

[6]Eric Jondeau (2010)

1.1.4 The Zumbach and Fernández (2013) Framework

The model adopted in this paper follows the work of Zumbach and Fernández (2013), the idea is to address the limitations of the classic BSM option pricing method. The approach is on the opposite side of the stochastic volatility models and tracks the path of pricing contingent claims in discrete time. This framework started with the work of Rubinstein (1976) and Brennan (1979), focused on the valuation of uncertain income streams. Rubinstein, in particular, generalized the Black and Scholes conditions for discrete models. The fundamental step was the pricing under the hypothesis of risk-neutral investors, thanks to the development of Risk Neutral Valuation Relationships (RNVRs). Using the RNVRs, it was possible to define the change from the physical $\mathbb{P}$ to the risk-neutral $\mathbb{Q}$ probability measure. Unfortunately, using a lognormal process for the underlying prices was ineffective, and the focus was moved to the research of a more realistic process. The ARCH model family was ideally suited for the scope, and more specifically, the GARCH[7] process has been widely used to determine the volatility dynamic. In this direction, Duan (1995) developed an option pricing model in the context of the generalized autoregressive conditional heteroskedastic (GARCH) for modeling the asset returns. The Duan paper follows Rubinstein and Brennan concerning the risk neutralization moving to a generalized version (adaptable to the GARCH process) termed "locally risk-neutral valuation relationship" (LRNVR). The issue lay in the distribution of innovations since a consistent change of measure was not possible for distributions that decay at a power law (such distributions usually better describe financial returns). The last crucial step forward comes from the Christoffersen et al. (2010) work introducing the change of measure $\frac{d\mathbb{Q}}{d\mathbb{P}}$, called Radon-Nikodym derivative, to move between the two measures. In this framework, Cristoffersen leaves the freedom to choose the underlying process with normal and nonnormal innovations.

Zumbach and Fernandez's option pricing model is a natural extension of the just-exposed existing pricing framework. The methods began with some premises:

- The model should describe the underlying behavior realistically, which is possible by including significant stylized facts.
- The model parameters must be estimated from historical information[8] so that the process can replicate the dynamics of different underlyings.
- The risk preferences must be considered, and the change of probability measure must be defined. The change of measure has to be consistent with different distributions.

In order to better capture the empirical findings in the financial markets, a finite time increment δt process has been set up. Following the path of their predecessors, Zumbach

[7] Bollerslev (1986)

[8] This is equivalent to saying that the filtration $\mathbb{F}$ must be updated to time t where the process simulations start.

and Fernandez rely on the ARCH family, augmenting the standard models to capture realistic dynamics. ARCH processes, specifically GARCH, have the flexibility to account for different specifications[9], we will use the Zumbach et al. (2014) multicomponent GARCH that will be better explained in the next chapter. This way, the underlying process can be defined to accommodate empirical observations such as fat-tails, negative skewness, heteroscedasticity, leverage effect, and more. On the root left by Cristoffersen, the change of probability measure is executed using the Radon-Nikodym derivative $\frac{d\mathbb{Q}}{d\mathbb{P}}$, and the method was augmented to account for different return distributions. In this context, the striking innovation was discovering an analytical method to compute the derivative without solving the expectations (integrals) along each underlying path. Due to this, the option price can be expressed as an expectation in the $\mathbb{P}$ measure, and the derivative allows an analytical transition to the $\mathbb{Q}$ measure. The risk aversion function must be specified since it does not arise naturally like in the BSM pricing scheme, and its dependence on the option price passes, precisely, through $\frac{d\mathbb{Q}}{d\mathbb{P}}$.

In conclusion, we can efficiently summarize the option pricing technique as in the original paper of Zumbach and Fernández (2013). Estimate the underlying parameters by selecting the favorite GARCH process. Then, setting up the filtration to the pricing date t_0 and simulating the underlying paths till option maturity. Compute the Radon-Nikodym derivative along each trajectory simulated with the Monte-Carlo and use it to weigh the option's payoffs at maturity. Lastly, perform the expectation for the discounted payoffs in the $\mathbb{P}$ measure.

1.1.5 American options

When we move into the American option pricing framework, we add complexity to the pricing challenge. Compared to their European counterparts, American options give holders the right but not the obligation to exercise the option at any time up to its expiration date. Bermuda, a variant of American options, allows early exercise only at predetermined dates before maturity. Thanks to this feature, pricing such derivatives may be complicated, usually with no closed-form solutions. Thus, numerical and simulation procedures are better suited for this scope. A first characteristic of the American and Bermuda options is that their price is always greater or equal compared with European.

The American option pricing focused on the pricing of put options because it is never optimal to early exercise a call on non-dividend paying stocks. We will use the J. C. Hull (2012) notation to explain this concept better. Let us consider two portfolios A and B, and two possible assets: an American call C with K strike and the underlying stock S. The

[9]The next section will dive deep into the stylized fact captured by the model.

portfolios composition is:

$$A = C, \ and \ K \ cash$$
$$B = S$$

The cash in the portfolio A earns the risk-free rate until it is used to exercise the call. The value of the portfolio B follows just the stock S, and by contrast, the portfolio A depends on the interests accumulated by the cash component. If we exercise early, the value of the portfolio A would be:

$$A_t = \ (S - K) + K(1 + r)^{T-t} \ < \ S = B, \ \ with \ t < \Delta T$$

and at the maturity T

$$A_{\Delta T} = \ \max(S - K, 0) + K(1 + r)^{T-T} = \max(S, K) \ \geq \ S = B,$$

so early exercise for an Americal call is never worth it. Beyond the mathematical proof, the reason behind it can be intuitive: one of the components of an option value is the time, and as we saw in the BSM formula, the value of an option is positively correlated with the time until expiration. Thanks to asymmetric option payoffs, the holder can benefit from stock price movements without committing capital by holding onto the option and not exercising it. However, it could be beneficial to early exercise an American put option. The reason is that the put options payoff is capped, and when the limit is almost reached, there may be the convenience to exercise and earn the cash risk-free rate. In reality, there are occasions where a call early exercise is desirable and depends on some holder or asset-specific factors. We will follow the arguments exposed by Natenberg (2014). In particular, the exception in which we may be willing to exercise a call option early is before a dividend payout of the underlying. We can break down the call option value into an intrinsic value, volatility value (the higher the volatility, the higher the price), and interest rate value since as the interest rate increases, the call would become preferable to holding the stock. On the opposite side, we have the dividend value, which has a negative relationship with the option value, and we can rewrite everything as: Call Value= intrinsic value + volatility value + interest value - dividend value. An early exercise could be convenient when the dividend value becomes preponderant, such as Dividend value > volatility value + interest value. The optimal moment to exercise is right before the dividend payment to maximize the call value, and there are no other situations where call early exercise might be convenient. For this reason, the development of an American call option pricing framework is not attractive since it entirely depends on dividend politics, which are firm-specific.

The contingent nature of American options makes it a natural choice to use the simulation paths approach to obtain the prices. The first widespread model was the Cox et al. (1979)

referred to as the "binomial option pricing model." It provides an intuitive, step-by-step method to determine option pricing and offers insights into the option's potential price paths. The binomial model assumes that an option's underlying stock price can move to only two possible prices over a short period: an "up" price and a "down" price. This simplifying assumption allows for the modeling of option pricing as a binomial tree of stock price movements, and the more the underlying process is repeated, the closer the value is to the real price. Although computationally more intensive than formulas like Black-Scholes, the model's flexibility and clarity make it a powerful tool. Another breakthrough is the Barone-Adesi and Whaley (1987), which tried to overcome the computational time problem of its predecessors. The idea was to combine the Black-Scholes European option pricing formula with a quadratic approximation for the early exercise premium (difference between American and European option prices), rendering the model more mathematically complex than the Binomial one. The Barone-Adesi and Whaley approximation is handy for pricing put options on stocks with constant or continuous dividend yields and provides a good trade-off between accuracy and computational efficiency.

1.1.6 The Least Square Montecarlo

The Least Square Montecarlo(LSM) by Longstaff and Schwartz (2001) implies a simulation-based approach and offers a way to estimate option values using simple regression techniques. The authors wanted to suggest an alternative approach to the previous models' binomial and finite difference techniques. Additionally, the LSM method shows the power of the simulation approach, which can be very flexible and accommodate many different types of financial derivatives.

The core of American option pricing is the optimal stopping problem, which means that the convenience of the early exercise must be determined at each time step. The option price is still the simple average of the discounted payoff, and the difficulty is to asses a rule for determining the value of the continuation and comparing it with the early exercise one. The algorithm works recursively, which means starting from the penultima time step, it compares the discounted conditional expected value of the continuation with the discounted value of the early exercise. The crucial passage and the model innovation were determining an efficient and robust rule to compute the expected value. Many models use a "brutal force" approach, which requires at each time step to recursively simulate again the underlying till maturity to asses the expectation. In contrast, the LSM proposed to compute such expectation with a linear regression between the ex-post payoffs from continuation with functions of the past simulated prices, computing a function that can approximate the continuation value. The continuation value for a random path ω is formally

reported in the original paper as:

$$F(\omega; t_k) = E^{\mathbb{Q}}\left[\sum_{j=k+1}^{K} \exp\left(- \int_{t_k}^{t_j} r(\omega, s) ds \right) C(\omega, t_j; t_k, T) | \mathbb{F}_{t_k} \right] \tag{6}$$

which is the conditional expectation in the risk-neutral measure of the future payoffs between the time t_k and t_j discounted at the risk-free rate. The procedure requires simulation of an underlying in the risk-free measure, such as a Geometric Brownian Motion with $\mu = r$, and recursively calculates the expectation at every k time step. To perform the expectation, the model implies doing a linear regression between the future payoffs and functions of the state variables.

$$\left.\begin{matrix} P(1,1) & P(1,2) & \cdots & P(1,N) \\ P(2,1) & P(2,2) & \cdots & P(2,N) \\ \vdots & \vdots & \ddots & \vdots \\ P(n-k,1) & P(n-k,2) & \cdots & P(n-k,N) \end{matrix}\right\} x$$

$$\left.\begin{matrix} K - P(n-k+1,1) & K - P(n-k+1,2) & \cdots & K - P(n-k+1,N) \\ \vdots & \vdots & \ddots & \vdots \\ K - P(n,1) & K - P(n,2) & \cdots & K - P(n,N) \end{matrix}\right\} Y$$

The linear regression is computed between Y and X:

$$X = [\overline{1},\ f_1(x),\ f_2(x) \ldots f_k(x)] \tag{7}$$

where f_k is the basis function polynomial chosen. The basis functions can be selected from various ranges, and in the original paper, the suggestions are between Laguerre, Hermite, Chebyshev, Legendre, and Jacobi polynomials.[10]LSM provides a flexible framework that accommodates underlying dynamics, handles path-dependent options, and adapts to various payout structures. However, the models have some downsides worth mentioning. The LSM method relies on path simulations, and when the underlying process is misspecified or unrealistic, the model might provide mispriced option valuations. When simulating price paths using the LSM approach, one has to ensure that the dynamics are specified under the risk-neutral measure. Despite this, real-world data, like historical stock prices, exist under the physical $\mathbb{P}$ measure. Specifying the risk-neutral distribution can be challenging for models with complex dynamics, like stochastic volatility or jump diffusion.

[10]Several other choices are possible.

1.2 Stylized facts and empirical findings

In the complex world of finance, empirical observations often reveal patterns and behaviors that deviate from classical financial theories. Termed "stylized facts," these empirical findings provide crucial insights into the actual dynamics of financial markets, often challenging and redefining the basic theoretical models. Furthermore, the accurate prediction and pricing of options demand more than just theory; it necessitates a deep understanding of market dynamics captured by stylized facts. The model approach that we will follow encapsulates these empirical pieces of evidence, trying to achieve an underlying process that can realistically replicate the behavior of the real one. We will now proceed to examine the empirical findings that the model addresses.

1.2.1 Heteroscedasticity

In financial markets, the assumptions of constant volatility and uncorrelated returns often prove to be oversimplified generalizations.The volatility clustering is a phenomenon that has been documented since at least the 1960s when it started to be considered a crucial aspect when financial returns are modeled. The basic idea is that large price changes tend to be followed by further large changes, regardless of the direction (up or down). Similarly, periods of small changes often precede more of the same.

There is no evident trend or pattern considering the financial returns series, and this characteristic can be supported by looking at the auto-correlograms associated with them.

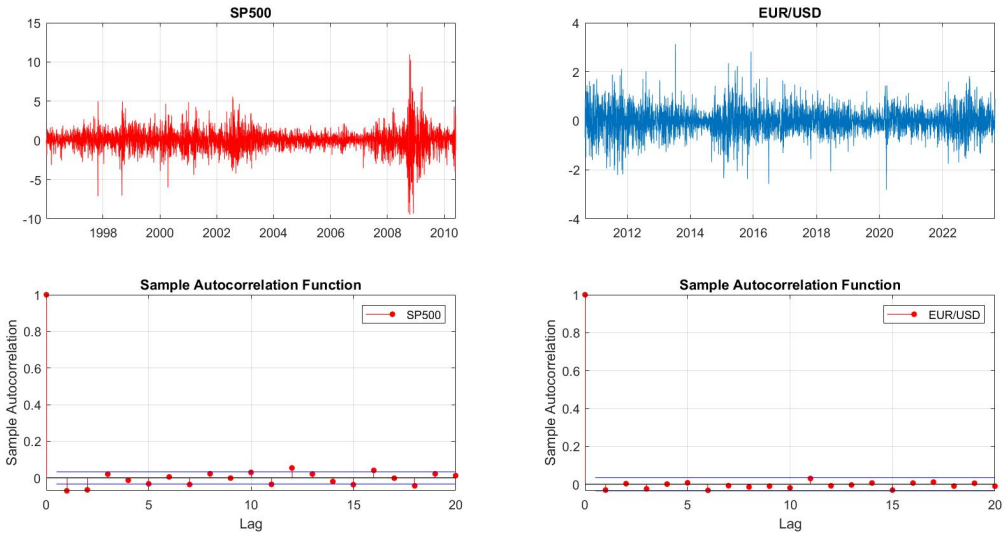

Figure 2: *Daily logarithmic returns for the SP500 and Eur/Usd time series and their autocorrelogram. Data source: Bloomberg*

Figure 2 shows that the correlation between returns instantly decays after the first lag. However, the situation changes when we move to squared returns (or returns in absolute

value $|r|$). The clustering of the volatility can be easily seen in Figure 3, and there is a clear alternation between high and low volatility periods.

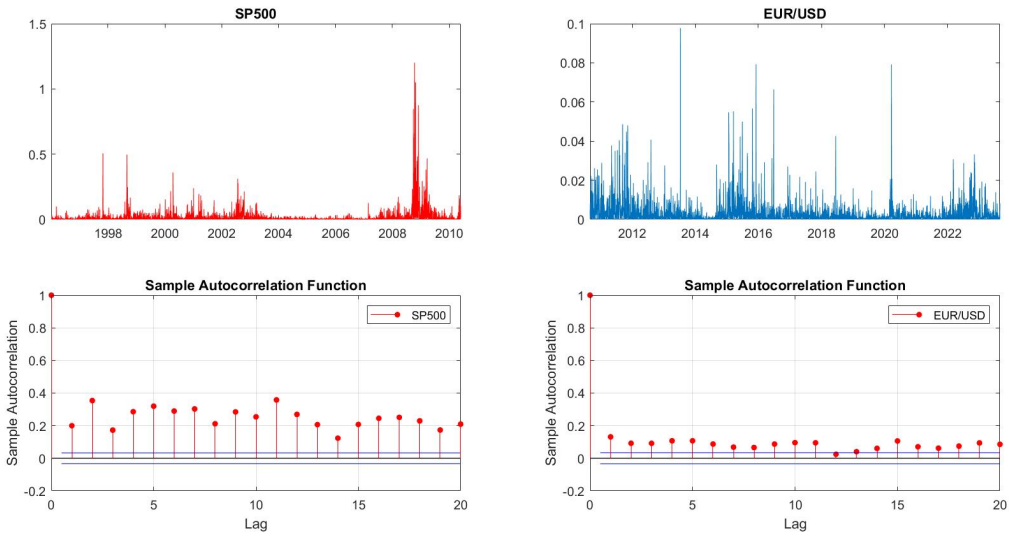

Figure 3: *Daily Squared logarithmic returns for the SP500 and Eur/Usd time series and their autocorrelogram. Data source: Bloomberg*

Moreover, the autocorrelations do not decay, showing persistency in the series. The idea is to capture this phenomenon by assuming the heteroscedastic behavior of the volatility. The models that assume constant volatility, like a simple ARMA model, cannot capture this phenomenon. The first model that formally encapsulates the volatility clustering is the milestone work from Engle (1982).

$$r_t = \sqrt{\sigma_i^2}\, z_i,\ z_i \sim \mathcal{D}(0,1) \tag{8a}$$

$$\sigma_i^2 = \alpha_1 r_{i-1}^2 + \alpha_0,\ r_i|\Omega_{i-1} \sim \mathcal{D}(0,\sigma_i^2) \tag{8b}$$

These equations are the fundamental building blocks for most variance deterministic heteroscedastic models. For this reason, the model we will use in this paper is an augmented form. Applying the ARCH model to the series, we can remove an essential part of the persistence in the squared return. As expected, the correlograms of the squared returns clearly show that the autocorrelations decay faster and stay at low levels (Figure 4). In conclusion, it is critical to understand and integrate heteroscedasticity and volatility clustering into our financial models to achieve more realistic and reliable option valuations.

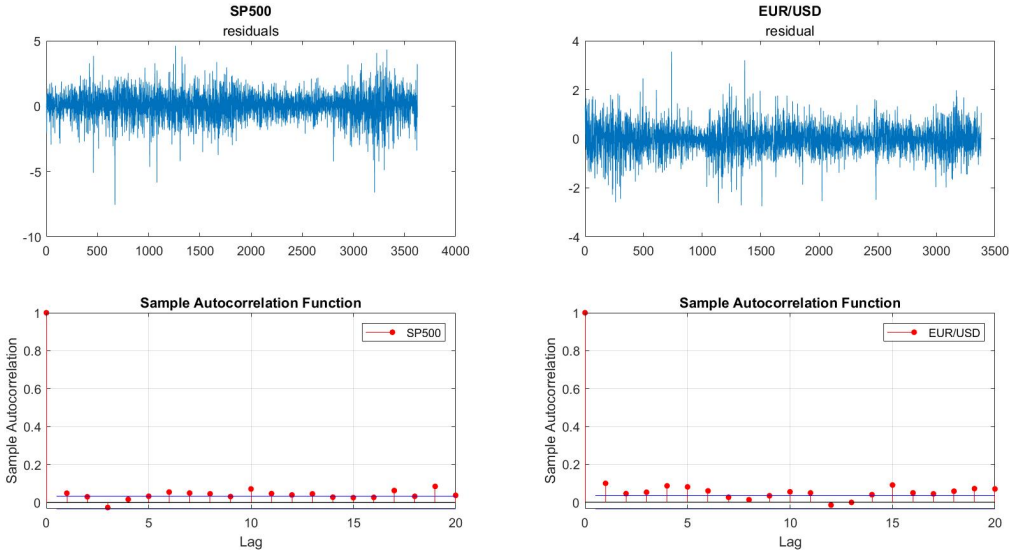

Figure 4: *SP500 and Eur/Usd residuals after applying ARCH(3) model. Correlograms of the squared returns after applying ARCH(3).*

1.2.2 Leverage effect

One of the most influential phenomena to consider is the leverage effect, which is the negative correlation between an asset's returns and its volatility. The name "Leverage" comes from one of its principal explanations: when a stock has a negative return, the level of equity decreases, and the debt remains constant, increasing the leverage ratio and the firm's riskiness. Consequently, the volatility increases more after a negative return than a positive one. This empirical observation has profound implications, particularly in option pricing, where volatility is a crucial determinant of option values. The family of ARCH models can easily accommodate this feature, again confirming the tool's strength. Specifications like GJR-GARCH, TARCH, or EGARCH are augmented versions of a classic GARCH(1,1) model that can capture the leverage effect using different methods. The news impact curve introduced by Engle and Ng (1993) is a convenient way to visualize this phenomenon. The paper aims to derive a tool to understand how new information is incorporated into volatility estimates. The news impact curve relates the past shocks(news) with the current level of volatility, showing the effect of negative shocks compared with the positive ones. As shown in Figure 5, the GARCH(1,1) model is symmetric and does not capture the leverage effect. Although the EGARCH model can grasp this effect, its news impact curve is entirely asymmetric, showing the significant impact of the negative shocks. Acknowledging and integrating the leverage effect into option pricing models is indispensable for achieving pricing accuracy. The model we will present accommodates this stylized fact through an ARCH model. The procedure allows us to incorporate a crucial characteristic of the financial markets to obtain a more realistic process.

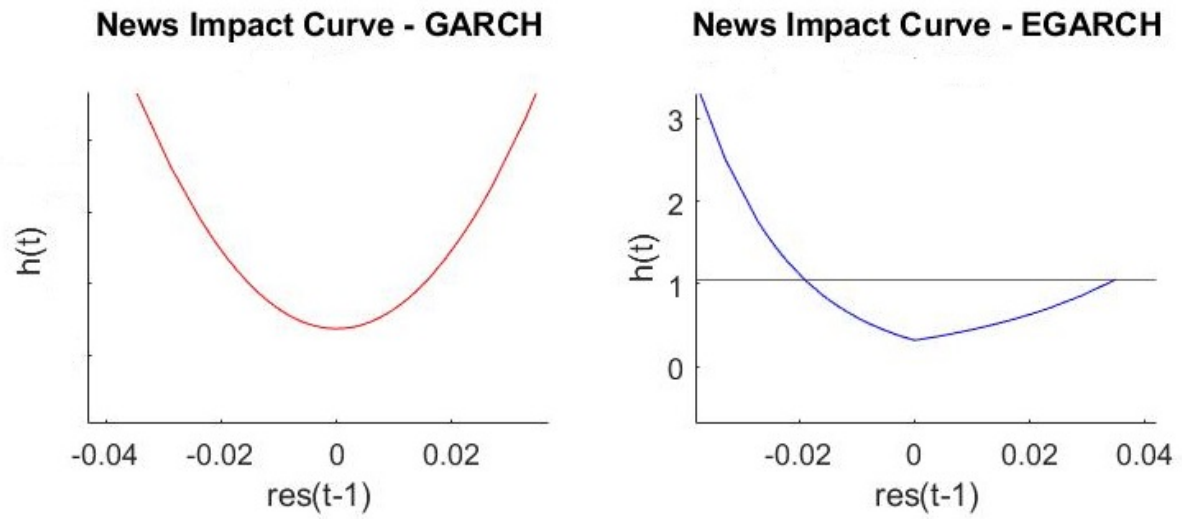

Figure 5: *News impact curves for the SP500. Where h(t) is the volatility*

1.2.3 Time reversal Invariance

The time reversibility assumption asserts that financial processes are statistically identical, whether observed forward or backward. A formal definition is that the transformation from t to $-t$ results in a symmetric system. This is why, looking at a financial return series, we cannot understand if it is going forward in time or vice versa. This phenomenon is usually associated with the physics laws that have this property, and even in finance, many processes are constructed considering time reversibility.

The time reversal invariance (TRI) was deeply analyzed by Zumbach (2009). The paper focuses on constructing several statistics that help understand if financial series have this property. A first achievement was noticing that the distribution of the volatilities is not symmetric, where a time-invariant process should have this feature. The paper concludes that financial time series are not time-invariant, and one of the key statistics used to assess it is the correlation of the volatility at different time horizons. Intuitively, this fact is not surprising since we know for a fact that investors have a memory of financial time series, and rarely can we consider them as true Random walk processes. For this reason, a realistic underlying process needs to account for this asymmetry. To accommodate the time reversal invariance(TRI) stylized fact, Zumbach proposed a multi-scale ARCH process that considers volatility at different time horizons. This process can capture the asymmetry in contrast with classic models like a simple GARCH(1,1).

1.2.4 Returns Distribution

One of the distinctive features observed in financial returns data is excess kurtosis. This statistical phenomenon, characterized by fat tails in the return distribution, means that positive and negative extreme events occur more frequently than expected by a normal distribution. Furthermore, accurate option pricing depends on a realistic assessment of the

distribution of underlying asset returns. When returns exhibit excess kurtosis, the standard assumption of a normal distribution falls. Option pricing models that account for fat-tailed distributions, such as the Student's t, can better capture the proper risk profile of financial derivatives.

We can deeply analyze this phenomenon following Zumbach (2013). The Gaussian distribution is usually used to model returns because of the central limit theorem. Since returns are uncorrelated, the daily returns, which are the sum of several elemental high-frequency returns, should tend to a Normal distribution. Despite this assumption, as we can see from Figure 6, the tendency to the Gaussian distribution is much slower than one day. This phenomenon happens because even if the returns are uncorrelated, the variances are not; therefore, the returns are not independent, and the consequence is an excess kurtosis slow decay.

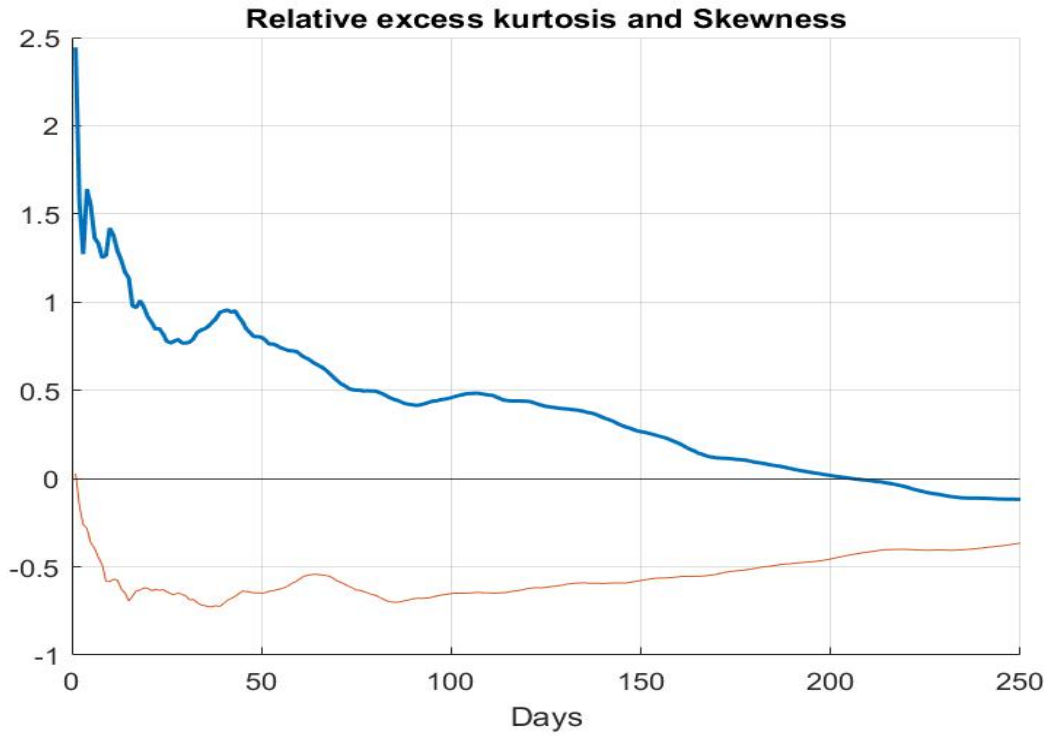

Figure 6: *Skewness and relative excess Kurtosis at increasing time intervals for SP500.*

One other distributional empirical find about returns is the negative Skewness. In general, Skewness measures the degree of asymmetry in a distribution; when it is negative, it means that the distribution of returns is skewed toward the left and is asymmetric. The Negative Skewness depends on the fact that huge drops in the stock market are more frequent than large-up movements. This explanation also means that financial returns that are symmetric in the drops, like exchange rates, do not show this stylized fact or, at least, is less pronounced.

To conclude the "Stylized facts" section, we want to state that the already explained phenomena are not the only ones captured by our process, but those are the more signif-

icant historically and in terms of correct simulation of the underlying. Recognizing and incorporating the stylized facts of financial markets into simulation models ensures a more realistic picture of underlying asset dynamics.

2 Methodology

The following chapter will explore the methodology employed in the thesis. The method we will present follows the Zumbach approach developed in different papers over more than a decade. We will pass through every model and technical implementation to achieve the option pricing. The approach aims to encapsulate the stylized facts, and we must carefully select the model characteristics. For example, the returns are relative and calculated over increasing time horizons to incorporate the empirical distributions. Moreover, the GARCH parameters are obtained through a calibration method to match the underlying features better. The chapter concludes with the model extension allowing us to price American Options. The last section diverges from the Zumbach methodology, exploring the implementation of the LSM method to expand the approach to the American options.

2.1 Returns

There are usually two ways to define financial returns.

$$logarithmic\ return : r_{log}(t) = \log(p(t)) - \log(p(t - \delta t)) \tag{9a}$$

$$relative\ return : r_{rel}(t) = \frac{p(t)}{p(t - \delta t)} - 1 \tag{9b}$$

Considering the findings of O'Neil and Zumbach (2009), we used relative returns instead of the most common logarithmic ones. The reason for this choice is to accommodate two crucial financial stylized facts: fat-tail distribution and negative skewness of the returns. The core of our pricing model is the Monte-Carlo simulation; when using a logarithmic random walk, several difficulties arise if we want to account for fat tails and negative skewness. It is possible to better explain the problem using the four arguments by O'Neil and Zumbach.

- Firstly, in the context of a logarithmic random walk, the expected price one period ahead requires solving the integral $E[\exp(\sigma\epsilon)]$ where the random process ϵ is associated with a distribution $p(\epsilon)$. For a valid computation of the expected price, the integral of $E[\exp(\sigma\epsilon)]$ must converge to a finite value. This convergence requires the distribution $p(\epsilon)$ to decay faster than an exponential function. The expected price can reach infinity, and if it does not, leading to an invalid result. Higher probabilities for extreme values characterize fat-tailed distributions, and while they often more realistically represent financial data, they pose problems in a logarithmic random walk. The integral diverges for any fat-tailed distribution, as they do not decay faster than an exponential function, rendering the computation for the expected price unworkable.

- Secondly, the problem of estimating volatility becomes more complex due to the exponential mapping, increasing the sensitivity to significant events. The exponential

function is highly sensitive to its input in a Monte-Carlo context. Even a slight increase in the input leads to a much more significant increase in the output. Applying the exponential function to a large draw will make it even larger, amplifying its effect. Because the exponential function boosts large values, it can have a pronounced effect on volatility measures.

- Thirdly, one significant empirical observation is the persistent negative skew in the log returns of stocks and stock indexes. This feature contrasts what would be expected under some traditional models. As a confirmation, logarithmic random walk with symmetric innovations describes many time series in financial markets. This means that, under such an assumption, the distribution of log returns should have zero skews. When log returns are modeled this way, relative returns follow a log-normal distribution, exhibiting positive skew. However, market data does not show this positive skew, presenting a significant contradiction.

- Our final argument follows from the work of Christoffersen et al. (2010), which "combining non-normal distributions and heteroskedasticity attempts to correct the biases associated with the conditionally normal GARCH model.". In order to construct the equivalent martingale measure, the characteristic function for the innovation distribution should exist. This means that $E[\exp(\sigma\epsilon)]$ should exist, which is possible, as mentioned before, almost only for normally distributed innovations and so, excluding fat-tailed distributions. However, we can use relative returns to derive the equivalent martingale measure for fat-tailed distributions. For this reason, a geometric process can accommodate the realistic features we want to include in our model.

2.1.1 Returns aggregation

Another realistic aspect we want to include in our model is the non-zero lagged correlation of returns. In order to include this feature, we need to estimate returns at different time horizons accordingly with Zumbach et al. (2014).

$$r[\Delta T](t) = \sqrt{\frac{1\ year}{\Delta T}}\ \frac{p(t) - p(t - \Delta T)}{p(t - \Delta T)} \tag{10}$$

Where $\Delta T = n\delta t$ and the returns are immediately annualized by the prefactor, which will help us calculate the volatility without scale problems. By doing this, we are creating a geometric returns process that can be expressed equivalently, starting from the returns at the δt scale:

$$r(t + \delta t) = \prod_{i=1}^{n} [1 + r_{rel}(t + i\delta t)] \tag{11}$$

We can transform a return at a δt scale to a ΔT scale by simply aggregating them. A more complex task is to do the same with the volatilities.

2.2 Volatility Estimation

In section 1.1.2, we highlighted the failure of the BSM model in capturing the characteristics of the implied volatility surface, like smiles, smirks, and term structure. These features depend on the underlying behavior, so we must find an accurate process to capture the underlying elements. In particular, we want to incorporate modern stylized facts, including fat-tailed distributions, heteroskedasticity, leverage effect, and aggregation at different time scales. Moreover, the process should allow us to change the measure from physical to risk-neutral. The selected price and returns processes are

$$p(t+\delta t) = p(t)(1 + \sqrt{\frac{\delta t}{1\ year}} r_{rel}[\delta t](t+\delta t))\,, \tag{12a}$$

$$r_{rel}[\delta t](t+\delta t) = \mu_{eff} + \sigma_{eff}(t)\epsilon(t+\delta t))\,, \tag{12b}$$

where σ_{eff} is the effective volatility that is the crucial component of our model. μ_{eff} represents the drift of the process or the mean return expected in the next period δt. We will investigate μ_{eff} in the following sections. ϵ is an iid random variable; accordingly to its distribution we will draw the process innovations. It has a distribution $p(\epsilon)$ with the following features: $E[\epsilon] = 0$ and $E[\epsilon^2] = 1$. $p(t)$ is the price at time t obtained from the geometric series of the annualized relative returns. Relative returns are at different timescales because of the return aggregation, so we have to annualize them according to it. Since $\delta t = 1\ day$ in our case, $1\ year = 260$ working days. Equations 12a and 12b define the basic structure of the model. Starting from them, we should define the parametrization of the effective variance.

2.2.1 GARCH(1,1)

Generalized Autoregressive Conditional Heteroskedasticity, commonly known as GARCH, has long been a fundamental model in time series analysis, particularly in financial econometrics. The GARCH(1,1) from Bollerslev (1986) and Engle is the model that historically has been the most successful in describing variance behavior. We would start from it to obtain a model that captures the stylized fact mentioned above. The classic GARCH(1,1) is usually written as follows.

$$\sigma^2_{eff}(t+\delta t) = \alpha_0 + \alpha_1 r^2(t) + \beta\sigma^2_{eff}(t)\,, \tag{13}$$

Following Zumbach (2002), we can rewrite Equation 13 incorporating an exponential moving average.

$$\sigma_1^2(t) = \mu\sigma_1^2(t-\delta t) + (1-\mu)r^2(t)\,, \tag{14a}$$

$$\sigma_{eff}^2(t+\delta t) = \sigma^2 + (1-w_\infty)(\sigma_1^2(t)-\sigma^2) = (1-w_\infty)\sigma_1^2(t) + w_\infty\sigma^2, \tag{14b}$$

Where the three parameters of interest are σ,w_∞ and μ. We can easily prove that Equations 14a and 14b are just a specification of Equation 13 in which $\alpha_0 = \sigma^2(1-\mu)w_\infty$, $\alpha_1 = (1-\mu)(1-w_\infty)$ and $\beta = \mu$. Intriguingly, in this format, the GARCH(1,1) process exhibits an internal variable, the historical volatility σ_1, written as an exponential moving average (EMA). Nothing has changed between Equations 13 and 14a-14b, but now we can better interpret the model parameters, especially when contrasting them against the standard α and β parameterization. The term involving w_∞ offers insight into mean reversion, a critical concept in finance. The equation showcases how the forecast is driven by a mean term, adjusted by the difference between historical volatility and mean volatility. This structure reveals the interaction between recent volatility and long-term average volatility, thus providing a clear picture of the mean-reverting nature of volatility. RM1996 by J.P.Morgan/Reuters (1996) introduced the use of the exponential moving average in the volatility estimation. The model became widespread for its simplicity by proposing a fixed decay factor of 0.94. In this respect, for the case where $w_\infty = 0$, the GARCH(1,1) equations conveniently simplify to:

$$\sigma_{eff}^2(t+\delta t) = \mu\sigma_{eff}^2(t) + (1-\mu)r^2(t), \tag{15}$$

Characterized by a single parameter μ, it resonates with the RiskMetric formula, especially when $\mu = 0.94$. The name of this model is I-GARCH(1).

2.2.2 Long Memory ARCH

With the classic GARCH models, we can capture the heteroskedasticity of the underlying variance. Following the Zumbach (2002) model, we use "a set of volatilities over increasing time horizons." In this way, we can also consider the variance long memory, particularly the volatility correlation at a logarithmic law. The volatilities show a non-zero lagged correlation, so it is crucial to incorporate past information to forecast future volatilities.

$$\sigma_k^2(t) = \mu_k\sigma_k^2(t-\delta t) + (1-\mu_k)\Big\{1 - \lambda_{lev}\tanh\left(\frac{r_k(t)}{\lambda_{range}\sigma_\infty}\right)\Big\}r_k(t)^2 \tag{16a}$$

$$\sigma_{eff}^2(t) = \sum_{k=1}^{n} w_k\sigma_k^2(t) + w_\infty\sigma_\infty^2, \tag{16b}$$

In the proposed variance estimation formula from Zumbach et al. (2014), special attention has been paid to adequately capture the pronounced leverage effect frequently observed

in financial markets. Our parametrization incorporates this feature through the inclusion of the hyperbolic tangent function. The scaling factor, λ_{lev}, acts as a leverage coefficient, modulating the model's sensitivity to the leverage effect. A larger value of λ_{lev} would imply a more pronounced response to the leverage effect and vice versa. The normalization factor,$\lambda_{range}\sigma_\infty$, ensures consistency of the return to the long-term or equilibrium volatility, σ_∞. As the Equation 15, the historical variance is computed by an exponential moving average(EMA) with the weights

$$\mu_k = \exp\Big(-\frac{\delta t}{\tau_k}\Big) \tag{17}$$

This way, we have introduced leverage and different time horizons in this formulation. After computing the historical variances $\sigma_k^2(t)$, the effective variance is computed as a convex combination between them and the long-term variance, σ_∞^2. The weights w_k are computed as $w_k = (1 - w_\infty)\chi_k$ where

$$\chi_k = \frac{1}{C}\left(1 - \frac{\log(\tau_k)}{\log(\tau_0)}\right) \tag{18}$$

with $\sum_k w_k = 1 + w_\infty$ and C is a normalization term fixed to ensure $\sum_k \chi_k = 1$. It is essential to notice the logarithmic decay of the weights, because the return's lagged correlations, would also decay logarithmic. As mentioned in Zumbach (2006), this is precisely the long-memory stylized fact observed in the financial returns we want to capture. The time intervals ΔT_k are built with a geometric progression of the form:

$$\tau_k = \frac{\tau_1}{\Delta T_1}\Delta T_k \tag{19a}$$

$$\Delta T_k = \Delta T_1 \rho^{k-1} \tag{19b}$$

The parameters are ρ, ΔT_1, τ_1, and τ_0, which must be selected accordingly with the underlying process.

2.2.3 Parameters estimation

The parameters are computed through a heuristic procedure reported in Zumbach et al. (2014). In particular, the approach uses a set of distributional properties estimators and adjusts the parameters to reproduce the distributional characteristic of the underlying. The calibration approach is on the opposite side compared to a Maximum likelihood estimation, and it is a more accurate method for our multi-scale necessities. The specific statistics used

are the l-estimators defined as follows:

$$l_1 = \binom{N}{1}^{-1} \sum_i r_i \tag{20a}$$

$$l_2 = \frac{1}{2}\binom{N}{2}^{-1} \sum_i \left\{ \binom{j-1}{1} - \binom{N-j}{1} \right\} r_i \tag{20b}$$

$$l_3 = \frac{1}{3}\binom{N}{3}^{-1} \sum_i \left\{ \binom{j-1}{2} + \binom{N-j}{2} - 2\binom{j-1}{1}\binom{N-j}{1} \right\} r_i \tag{20c}$$

$$l_4 = \frac{1}{4}\binom{N}{4}^{-1} \sum_i \left\{ \binom{j-1}{3} - \binom{N-j}{3} - 3\binom{j-1}{2}\binom{N-j}{+} 3\binom{j-1}{1}\binom{N-j}{2} \right\} r_i \tag{20d}$$

Where the four formulas are linear estimations for the distribution moments. L-moments are linear combinations of order statistics analog to conventional moments. Their robustness comes from their resistance to outliers and ability to describe distributions with tails that might deviate from Gaussianity. From such estimators, we can define L-moments as:

$$S_L = \sqrt{\pi}\, l2, \quad \tau_L = l_3/l_2, \quad k_L = \frac{1}{0.1226}\,\frac{l_4}{l_2} \tag{21}$$

which are, respectively, L-size, L-skew, and L-Kurtosis. Similarly, we compute the moments for the volatility: mean μ_σ, variance s_σ^2, and shape γ_σ. The statistics are on the sample and can be used to reference the volatility distribution. Defining $\langle\cdot\rangle$ the sample mean, the volatility statistics are computed as follows:

$$\mu_\sigma = \langle\sigma\rangle, \quad s_\sigma^2 = \langle(\sigma - \mu_\sigma)^2\rangle, \quad \gamma_\sigma = \frac{S_\sigma}{\mu_\sigma}, \tag{22}$$

The approach is an iterative refinement with repeated simulation and comparison. The idea is to fine-tune the GARCH parameters each time until the L-moments of the model closely match those of the empirical data.

2.2.4 Volatility Forecast

Forecasting volatility is critical for various applications in financial econometrics, from risk management and portfolio optimization to the pricing of derivative instruments. Given the difficulties and complexities embedded in financial markets, a model's efficacy is largely determined by its ability to capture real-world phenomena, such as long memory and heteroscedasticity. In the following sections, we delve into the mechanics of volatility forecasting using our proposed model. The theoretical model we will expose follows Zumbach's two already-mentioned papers: Zumbach (2002) and Zumbach (2006).

The forecast essential parameters are the lower cut-off τ_1, the upper cut-off τ_{max}, and

the decay factor τ_0. The lower cut-off τ_1 is a crucial parameter because, on the one hand, most of the information is in the recent values; on the other hand, including many recent values could result in a noise estimator that does not correctly include the long memory feature. Concerning the last parameter, the upper cut-off oscillates from a few months to a few years. So our key set of parameters is $\theta = [\tau_1, \tau_0, \tau_{max}]$. The variance forecast at time t given the filtration $\Omega(t)$ is provided by the conditional expectation till time $t + k\delta t$. In particular, we can express our conditional expectation as:

$$E[\sigma_k^2(t + j\delta t)|\Omega(t)] = \mu_k \; E[\sigma_k^2(t + (j-1)\delta t)|\Omega(t)] + (1 - \mu_k) \; E[\sigma_{eff}^2(t + j\delta t)|\Omega(t)] \quad (23a)$$

$$E[\sigma_{eff}^2(t + (j+1)\delta t)|\Omega(t)] = \sigma^2 + \sum_k w_k \Big\{ E[\sigma_k^2(t + j\delta t)|\Omega(t)] - \sigma^2 \Big\} \quad (23b)$$

When forecasting volatility, the gold standard for assessing the accuracy of predictions is to compare them with the realized one. By comparing our forecasts with this benchmark, we can measure the efficacy of our model in replicating actual market dynamics. The realized volatility is defined as:

$$\sigma_{real}^2 = \frac{1}{k} \sum_{j=1}^{k} r^2[\delta t](t + j\delta t) \quad (24)$$

Evaluating the quality of these forecasts necessitates a robust metric; for this task, we used the root mean square error (RMSE). The RMSE quantifies the average magnitude of the errors between predicted and observed values, offering a clear and interpretable measure of forecast accuracy. Mathematically, it is the square root of the average of squared differences between prediction and actual observation. A lower RMSE indicates a better fit of the model to the data, signifying more accurate volatility forecasts.

$$RMSE[T, \theta]\Big(\sqrt{\overline{F}\;[\sigma_{eff}^2]}, \sigma_{real}\Big) = \sum_t \left(\sqrt{\overline{F}\;[T, \sigma_{eff}^2](t)} - \sigma_{real}[T](t) \right)^2 \quad (25)$$

where $\overline{F}$ is the mean forecast variance between t and T and is defined as

$$\overline{F}[T, \sigma_{eff}^2](t) = \frac{1}{k} \sum_{j=1}^{k} F[j\delta t, \sigma_{eff}^2](t) \quad (26)$$

with $T = k\delta t$. Zumbach used the RMSE optimization instead of a log-likelihood estimate not to have distributional assumptions. In Zumbach (2006), L1 and L2 distances were used instead of RMSE. We tried all three estimates, but the results were very similar. For this reason, we are presenting only the root mean square error formula.

2.3 Model Drift

Estimating the drift μ has the scope to uncover the tendency or directionality of a financial asset or economic indicator. While volatility captures the randomness or uncertainty around this tendency, the drift can be seen as the "heartbeat" of the process. The estimation of the drift of the process is fully described in Zumbach and Fernández (2013), and in the subsequent section, we will delve into the methodology for drift estimation.

Estimating μ is a challenging task, and explaining why we would follow the arguments from Zumbach (2012), particularly the use of "plausible economic arguments." One of the pivotal concepts of financial economics is the risk-return tradeoff: riskier assets should, on average, offer higher returns as compensation for that risk. Risk-free assets, which carry no default risk, must yield lower returns, reflecting their stability. When we think of drift, particularly in the context of stock prices or returns, it is more than just a statistical parameter; it represents the expected return on the asset. Choosing a static drift would imply that this expectation remains constant over time, while adopting a time-varying drift aligns with this economic intuition. By allowing the drift to change with market conditions, we acknowledge the changing dynamics of risk and return in financial markets. Looking at the risk-free rate and the market risk premium over our period of interest[11], it is clear that the premium should be correlated to them and could not be static. Furthermore, the drift must be correlated with the volatility of the underlying, and following these arguments, Zumbach and Fernández (2013) ended up with a drift of this form :

$$\mu = r_{rf} - q + \beta \ln\Big(1 + \frac{\tilde{\sigma}}{\sigma_{rp}}\Big) \tag{27}$$

$\tilde{\sigma}$ is the volatility forecast, as proposed in section 9, for the next six months. β and σ_{rp} are the parameters used to fix the risk premium associated with volatility.

2.4 From Physical to Risk-Neutral probability measure

In quantitative finance, changing probability measures is one essential mathematical tool that allows us to bridge real-world observations with the theory. This concept is crucial when transitioning from the physical $\mathbb{P}$ (real-world) probability to the $\mathbb{Q}$ risk-neutral measure. The physical measure represents the actual probabilities of different market scenarios, as observed in real-world markets. It is grounded in historical data and actual market movements. In contrast, the risk-neutral measure is a hypothetical construct. Under this measure, all assets are expected to grow at the risk-free rate due to the investors' risk neutrality. By working under that measure, the transition to the risk-neutral simplifies option pricing: the expected return on an asset is the risk-free rate, and we can use it to

[11] 27

discount the option payoffs[12]. To fill the gap between these two measures, we introduce the Radon-Nikodym derivative. Mathematically, if $\mathbb{Q}$ is the risk-neutral measure and $\mathbb{P}$ is the physical measure, the Radon-Nikodym derivative, denoted $\frac{d\mathbb{Q}}{d\mathbb{P}}$, gives us the factor by which we adjust expectations under the physical measure to obtain expectations under the risk-neutral measure. In other words, we can express the option price as an expectation in the $\mathbb{Q}$ measure or, equivalently, in the $\mathbb{P}$ measure weight with the Radon-Nikodym derivative. In the forthcoming sections, we will go deeper into the Radon-Nikodym derivative, Market Price of Risk, and Equivalent Martingale Measure.

2.4.1 Equivalent Martingale Measure (EMM)

Considering a sequence of random variables $X_0, X_1, ...X_t, ...X_n$, we can defining it a Martingale if $E[X_{t+i}|\Omega(t)] = X_t$.[13] Given that definition, the expectation of every future value, considering the filtration $\Omega(t)$, is equal to today's value. It is easy, from the definition, to asses that the Martingale is a process with zero drift, and we can conveniently use this property for option pricing purposes. We want to use these properties to construct the so-called Equivalent Martingale Measure(EMM). Using the J. C. Hull (2012) notation, we will consider two securities prices f and g, dependent on a single source of uncertainty. Now let us define $\omega = \frac{f}{g}$, which is the relative price of f with respect to g. For some specific choices of the market price of risk, the equivalent martingale measure findings show that ω is a Martingale when there are no arbitrage opportunities. The following section will show how this finding fits our option pricing model and how to construct the EMM measure for Garch processes using the Radon-Nykodim derivative.

Constructing an EMM, we must start by defining a risk aversion function. We can skip this part using logarithmic returns since such returns are time-additive, meaning the log return over multiple periods is just the sum of the log returns of each base period δt. Basically, we are applying an exponential map when we move from simple to logarithmic returns. In our case, the exponential mapping that rises naturally with logarithmic returns is substituted with an arbitrary function with specific characteristics. "The risk aversion function $f(z)$ quantifies the adversity toward the future events as seen by the option writer," Zumbach and Fernández (2013).

The function is defined over the positive line $f(z) : \mathbb{R}^+ \to \mathbb{R}^+$ and it is a decreasing function. When shifting from the real world ($\mathbb{P}$) to the risk-neutral world ($\mathbb{Q}$), we need a mechanism to adjust for risk preferences. Here, the risk aversion function becomes pivotal. This function encapsulates how investors feel about risk by weighing the random events

[12] J. C. Hull (2012)
[13] Given that $E[|X_t|] < \infty$

differently. Now we can introduce the Radon-Nykodim derivative for a given sequence ν_i

$$\frac{d\mathbb{Q}}{d\mathbb{P}}\bigg|\mathbb{F}_n = \prod_{i=0}^{n} \frac{f(\nu_i z_{i+1})}{E_i^{\mathbb{P}}[f(\nu_i z_{i+1})]} \tag{28}$$

where $E_i^{\mathbb{P}}[f(\nu_i z_{i+1})]$ is a normalization function for $f(z)$ with $\nu_i > 0$. The normalization is positive given the positivity conditions on z, f, and ν. Now we can use $\frac{d\mathbb{Q}}{d\mathbb{P}}$ to change the measure from $\mathbb{P}$ to $\mathbb{Q}$, specifically $E^{\mathbb{Q}}[\cdot] = E^{\mathbb{P}}\left[\frac{d\mathbb{Q}}{d\mathbb{P}}\right]$. A convenient choice for the risk aversion function is $f(z) = \exp(-z)$; we can call the derivative Esscher transform using it. Christoffersen et al. (2010) shows that different functions $f(z)$ can be used to construct the EMM. For Taylor expansion purposes, which we will better explain in the following section, our final solution is $f(z) = \frac{1}{1+exp(z)}$, which shows a smother decay. As mentioned, we need to introduce a new price process to construct an equivalent martingale measure and ω. Let us consider a market (S, B) where S is our stock process, and B will be specified later. We start in the space $(\Omega, \mathbb{F}, \mathbb{P})$, and we will characterize a new probability measure $\mathbb{Q}$ equivalent[14] to $\mathbb{P}$. The new measure is to be such that the normalized price processes are Martingales. Now introducing a generic *numeraire* Y, and follows Pascucci (2011) we can define our EMM as the probability $\mathbb{Q}$ on $(\Omega, \mathbb{F})$:

$$\frac{S_i}{Y_i} = E^{\mathbb{Q}}\left[\frac{S_{i+1}}{Y_{i+1}}\bigg|\mathbb{F}_i\right], \frac{B_i}{Y_i} = E^{\mathbb{Q}}\left[\frac{B_{i+1}}{Y_{i+1}}\bigg|\mathbb{F}_i\right] \tag{29}$$

Considering the case where $Y = B$ we are back in the situation explained at the beginning of the section where $\omega_i = \frac{S_i}{B_i}$. If $\mathbb{Q}$ respects the EMM properties then

$$\omega_i = E^{\mathbb{Q}}\Big[\omega_n|\mathbb{F}_i\Big], i < n \tag{30a}$$

$$E^{\mathbb{Q}}[\omega_n] = E^{\mathbb{Q}}\Big[E^{\mathbb{Q}}[\omega_n|\mathbb{F}_0]\Big] = \omega_0 \tag{30b}$$

From this, we can see why it is a risk-neutral measure: the expectations normalized future prices are equal to today's. Therefore, A hypothetical investor would remain neutral, without inclination to buy or sell the assets. Consequently, $\mathbb{Q}$ is often termed as the risk-neutral probability. Now we can introduce our second price process B, which is a risk-free bond such as $B_{i+1} = B_i(1 + r_{rf})$. The process is a Martingale that can be defined as we did before $\frac{S_i}{B_i} = E^{\mathbb{Q}}\left[\frac{S_{i+1}}{B_{i+1}}\bigg|\mathbb{F}_i\right]$ or equivalently $1 = E^{\mathbb{Q}}\left[\frac{S_{i+1}}{S_i}/\frac{B_{i+1}}{B_i}\bigg|\mathbb{F}_i\right]$. We should underlie that both processes are in the $\mathbb{P}$ measure and contained in the filtration up to time i as well as σ_i, μ_i, r_{rf}. The conditions exposed in Equation 29 allow us to obtain an

[14]They have same null $\{\omega : \mathbb{P}(\omega) = 0\}$=$\{\omega : \mathbb{P}(\omega) = 0\}$ and certain events

ν_i equation in the $\mathbb{P}$ measure

$$\frac{E_i^{\mathbb{P}}[z_{i+1}f(\nu_i z_{i+1})]}{E_i^{\mathbb{P}}[f(\nu_i z_{i+1})]} = 1 - \mu_i + r_{rf} = 1 - \phi_i \sigma_i^2 \tag{31}$$

where ϕ is the risk premium factor defined

$$\phi_i = \frac{\mu_i - r_{rf,i}}{\sigma_i^2} \tag{32a}$$

and the subsequent market price of risk following Zumbach (2012) is

$$\lambda_i = \frac{\mu_i - r_{rf,i}}{\sigma_i} \tag{32b}$$

When $\mu_i > r_{rf}$, the risk premium ϕ is positive. We need to impose some restrictions on f, in particular, f should decay fast enough to guarantee that the left-hand side of Equation 31 is less than 1. The function we introduced before is a convenient choice to ensure it.

Thanks to this framework, we can map the change of measure from $\mathbb{P}$ to $\mathbb{Q}$, solving some integral equations along each path of the Monte Carlo simulation. Even if this theoretical approach is very convenient, some practical or computational difficulties may arise. More specifically, solving the integral along each path may result in computational problems. The following section will be dedicated to solving these problems, showing one of the Zumbach pricing scheme's most significant results.

2.5 Small δt expansion

One of the most remarkable intuitions from the Zumbach works is the analytical derivation of Equation 28. As we mentioned, solving the implicit equation given by this integral is a difficult task; the analytical derivation allows the model to solve a simplified equation along each path. The simplification is performed with a systematic Taylor expansion on $\sqrt{\delta t}$. The dependence between the previous derivation of the Radon-Nykodim derivative and δt was embedded in σ and μ that are scaled on that term.

We used a second-order Taylor polynomial $f(x) = f(a) + f'(a)(x-a) + \frac{1}{2}(a)(x-a)^2$, and to quantify the error of this approximation, we introduce a remainder term $\frac{1}{3!}f'''(\xi)(x-a)^3$.[15] Conceptually, the Taylor polynomial approximates f near $x = a$, and the remainder term represents the error between the polynomial and the true function. So, when we expand at δt we obtain

$$\begin{aligned} f(\nu z) = f(\nu(1+\sigma\epsilon)) &= f + \sigma\epsilon\nu f' + \frac{1}{2}(\sigma\epsilon\nu)^2 f'' + \frac{1}{3!}(\sigma\epsilon\nu)^3 f'''(\xi) \\ &= f\Big(1 + \sigma\epsilon\nu\frac{f'}{f} + \frac{1}{2}\sigma^2\epsilon^2\nu^2\frac{f''}{f} + O(\sigma^3)\Big) \simeq \Big(1 - \sigma\epsilon f_1 + \frac{1}{2}\sigma^2\epsilon^2 f_2\Big) \end{aligned} \tag{33}$$

[15] with ξ real value between a and x. The Lagrange form of the remainder guarantees that such ξ exists according to the mean value theorem.

where

$$f_1(\nu) = -\nu\frac{f'}{f},\ f_2(\nu) = \nu^2\frac{f''}{f} \tag{34}$$

and all the functions f with their derivatives are evaluated at ν. The function $f_1(\nu)$ is positive given that $f(\nu)$ is a decreasing function by the previous definition. Now we are ready to compute the expectations $E[f(z\nu)]$ and $E[zf(z\nu)]$:

$$E[f(z\nu)] \simeq f\Big(1 + \frac{\sigma^2 f_2}{2}\Big),\ E[zf(z\nu)] \simeq f\Big(1 + \sigma^2\Big(\frac{f_2}{2} - f_1\Big)\Big) \tag{35}$$

We can substitute the results into Equation 31

$$\frac{E_i^{\mathbb{P}}[z_{i+1}f(\nu_i z_{i+1})]}{E_i^{\mathbb{P}}[f(\nu_i z_{i+1})]} = 1 - \mu_i + r_{rf} = 1 - f_{1,i}\sigma_i^2 \tag{36}$$

and it is clear now that solving for ν_i we obtain $f_1 = \phi = \frac{\mu_i - r_{rf}}{\sigma_i^2}$. This result shows that the choice of the risk aversion function does not influence the f_1 term, but it only does on f_2. Furthermore, as we will see later, the fact that $f_1 = \phi$ is one reason why the option pricing scheme is quite robust against the choice of the risk aversion function. Following the same argument, ν is only used to compute f_2. Given this practical result, we can quickly and analytically derive the Radon-Nikodym derivative.

Considering a generic time to maturity T, the final price for the underlying is given by the stock process

$$S_n = S_0\prod_{i=0}^{n-1}(1 + \mu_i + \sigma_i\epsilon_{i+1}) = F_n\prod_{i=0}^{n-1}\Big(\frac{1 + \mu_i + \sigma_i\epsilon_{i+1}}{1 + r_{rf}}\Big) \tag{37}$$

where F_n is the forward price at the maturity T calculated in t_0. From this definition, we can perform a Taylor expansion, where the order of such expansion is $O(\delta t)$.

$$\begin{aligned} S_n &= F_n\prod_{i=0}^{n-1}\Big(1 + \mu_i - r_{rf} + \sigma_i\epsilon_{i+1} + O(\delta t^2)\Big) \simeq F_n\Big(1 + \sum_i(\mu_i - r_{rf}) + \sigma_i\epsilon_{i+1} + \sum_{i<j}\sigma_i\epsilon_{i+1}\sigma_j\epsilon_{j+1}\Big) \\ &\simeq F_n\Big(1 + \sum_i\sigma_i\epsilon_{i+1} + \frac{1}{2}\Big(\sum_i\sigma_i\epsilon_{i+1}\Big)^2 + \sum_i(\mu_i - r_{rf}) - \frac{1}{2}\sum_i\sigma_i^2 + \epsilon_{i+1}^2\Big) \end{aligned}$$

Now we can define

$$R = \sum_{i=0}^{n-1}\sigma_i\epsilon_{i+1},\ y = \sum_{i=0}^{n-1}\sigma_i^2(\epsilon_{i+1}^2 - 1),\ \sigma_{int}^2 = \sum_{i=0}^{n-1}\sigma_i^2 \tag{38}$$

so we can rewrite everything

$$\simeq F_n\Big(1 + R + \frac{R^2}{2} + \sum_i(\mu_i - r_{rf}) - \frac{y}{2} - \frac{\sigma_{int}^2}{2}\Big) \tag{39}$$

in which R is the stock path innovation and σ^2_{int} is the integrated variance. These elements will be fundamental during the Monte-Carlo simulation, and we can directly use these formulations to estimate them analytically. Once we did it for the price, the same needs to be done for the derivative

$$\frac{d\mathbb{Q}}{d\mathbb{P}} \simeq \prod_{i=0}^{n-1}\Big(1 - f_{1,i}\sigma_i\epsilon_{i+1} + \frac{1}{2}f_{2,i}\sigma_i^2\Big\{\epsilon_{i+1}^2 - 1\Big\}\Big) \tag{40}$$

expanding it to δt and defining the new measure-based path stock innovation and integrated variance

$$\begin{aligned}
&\simeq 1 - \sum_{i=0}^{n-1}\Big(f_{1,i}\sigma_i\epsilon_{i+1} + \sum_{i<j} f_{1,i}\sigma_i\epsilon_{i+1}\Big)(f_{1,j}\sigma_j\epsilon_{j+1}) + \frac{1}{2}\sum_i f_{2,i}\sigma_i^2\{\epsilon_{1+i}^2 - 1\} \\
&\simeq 1 - \sum_i f_{1+i}\sigma_i\epsilon_{1+i} + \frac{1}{2}\Big(\sum_i f_{1+i}\sigma_i\epsilon_{1+i}\Big)^2 + \frac{1}{2}\sum_i f_{2,i}\sigma_i^2\{\epsilon_{1+i}^2 - 1\} - \frac{1}{2}\sum_i f_{1,i}^2\sigma_i^2\epsilon_{1+i}^2
\end{aligned}$$

so we can define again

$$\tilde{R} = \sum_{i=0}^{n-1}\sigma_i\epsilon_{i+1}f_{1,i} = \sum_{i=0}^{n-1}\lambda_i\epsilon_{i+1},\ \tilde{y} = \sum_{i=0}^{n-1}\sigma_i^2(\epsilon_{i+1}^2 - 1)f_{2,i},\ \tilde{\sigma}^2_{int} = \sum_{i=0}^{n-1}\sigma_i^2 f_{1,i}^2\epsilon_{i+1}^2 \tag{41}$$

as we did before, we can rewrite the derivative using these new terms:

$$\frac{d\mathbb{Q}}{d\mathbb{P}} \simeq 1 - \tilde{R} + \frac{\tilde{R}^2}{2} + \frac{\tilde{y}}{2} - \frac{\tilde{\sigma}^2_{int}}{2} \tag{42}$$

This outcome is a O'Neil and Zumbach (2009) pivotal achievement, enabling us to implement the change in probability measure numerically. We calculated the expectation using a small δt expansion, crucial for incorporating the underlying realistic features. We can use the ARCH process introduced before at regular time increments (δt) because a continuum limit is unnecessary. To complete the framework, we need to define ν. We can do it by Equation $f_1(\nu_i) = \frac{\mu_i - r_{rf}}{\sigma_i^2}$. The solution is

$$\nu_{n+1} = \phi(1 + \exp(-\nu_n)) \tag{43}$$

solving for the function $f(z) = \frac{1}{1+\exp(z)}$.

Before concluding, we want to underline that even if the choice of the risk aversion function (f) is not a game-changing factor in option pricing, we should be careful when we deal with fat-tailed distributions. In particular, the relation between z and ν must be understood better. When z is small and ν large enough, "the exponential function overtakes the decrease of the Student distribution" Zumbach and Fernández (2013). Due to the convergence problem, we need to find a function with slower variations with respect

to a simply exponential function. In particular, the choice of a function like $f(z) = \frac{1}{1+\exp(z)}$ leads to good results[16]. In the previous sections, we established the essential framework for an accurate Monte Carlo simulation. The succeeding section will integrate these base concepts and expose how to execute the simulations.

2.6 Monte-Carlo Simulation

Monte Carlo simulation is a powerful computational technique that leverages randomness to solve problems that might be deterministic. Once we have a robust volatility estimate, Monte Carlo simulation allows us to simulate the potential future paths an underlying asset might take. Doing so multiple times can create a distribution of possible outcomes, providing a holistic view of potential scenarios. Once we have computed all the parameters for the underlying process, the basic idea is to simulate several paths accordingly with such parameters. The simulation is driven by the previously exposed process (Equations 12a and 12b), where the innovations follow a t-distribution with ν degrees of freedom. The t-student distribution, often called the t-distribution, is a compelling alternative to the standard normal distribution, mainly when modeling financial returns with fat tails. At the end of each simulation, the Radon-Nikodym derivative is computed analytically using Equation 42. One crucial aspect is to update the filtration of the underlying process up to t_0, which is the time we start our Montecarlo. After each time step δt, we should do the same and embed the previous time volatility in the computation for the subsequent one.

We used an antithetic scheme, a Montecarlo method used for symmetric distributions, to reduce the variance of the price estimator. The antithetic variates technique is a variance reduction method, which means it aims to reduce the variability or "noise" in the Monte Carlo estimations without needing more random samples. Following Jaeckel (2002), the paths are generated from symmetric innovations $\{z_i\}$ and $\{-z_i\}$. The idea is to average the two random samples functions into one, where

$$\tilde{v}(z_i) = \frac{\{v(z_i)\}+\{v(-z_i)\}}{2} \tag{44}$$

and the draws $\tilde{v}_i$ are independent. The scheme makes it possible to have an overall variance reduction $V[\tilde{v}_i] < \frac{V[v_i]}{2}$.

2.7 Option Pricing

The pricing of a European contingent claim at a generic date t_i between t_0 and the maturity T is given by the discount expectation of the option terminal value under the Equivalent

[16]The two functions' comparison can be graphically seen in Figure 4.

Martingale Measure(EMM) $\mathbb{Q}$:

$$C_i = E^{\mathbb{Q}}\left[C_n(S_n)\frac{B_i}{B_n}\Big|\mathbb{F}_i\right] = E^{\mathbb{P}}\left[C_n(S_n)\frac{B_i}{B_n}\frac{d\mathbb{P}}{d\mathbb{Q}}\Big|\mathbb{F}_i\right], \quad n = T \tag{45}$$

this formulation was first introduced by Christoffersen et al. (2010). The formula offers a rigorous and mathematically consistent methodology for option pricing by straddling between the real-world and risk-neutral probabilities. Furthermore, this pricing formulation is valid for every underlying process. At its core, this formula is not just about numbers; it embodies a fundamental economic principle: the absence of arbitrage opportunities. The justification of the formula using the no-arbitrage argument is stated in Zumbach (2013) and follows the idea that no arbitrage strategies can be constructed from a martingale portfolio; now, we will examine it thoroughly. In the previous section, we have defined $\omega = S_i/B_i$ as the discount stock where the numeraire is the bond. The option value at time i for ω

$$C_i^{\omega} = E^{\mathbb{Q}}[C_n^{\omega}(S_n)|\mathbb{F}_i] \tag{46}$$

applying the law of iterative expectation for $s < t$

$$C_i^{\omega} = E^{\mathbb{Q}}[C_n^{\omega}(S_n)|\mathbb{F}_i] = E^{\mathbb{Q}}\left[E^{\mathbb{Q}}[C_n^{\omega}(S_n)|\mathbb{F}_s]\Big|\mathbb{F}_i\right] = E^{\mathbb{Q}}[C_i^{\omega}|\mathbb{F}_i]$$

doing that Zumbach shows that also C^{ω} is a Martingale. In order to demonstrate the no-arbitrage argument, we need to introduce trading strategies and determine if profits can be made without risk.

2.7.1 No Arbitrage Principle

The available assets are three: the option(C), the stock(S) and the Bond(B). Now, let us denote the value of a hypothetical portfolio at time i as V_i. The portfolio can comprise different quantities of our three assets

$$V_i = \rho_i S_i + \gamma_i C_i + \beta_i B_i \tag{47}$$

where ρ, γ and β are the associated weights. The change in V_i value one step forward in time is

$$\begin{aligned}\Delta V_{i+\delta t} &= \rho_i(S_{i+\delta t} - S_i) + \gamma_i(C_{i+\delta t} - C_i) + \beta_i(B_{i+\delta t} - B_i) \\ &= \rho_i \Delta S_{i+\delta t} + \gamma_i \Delta C_{i+\delta t} + \beta_i \Delta B_{i+\delta t}.\end{aligned} \tag{48}$$

The quantity ΔV can be seen as the portfolio's gain (G) at each time step. Consequently, we can see the value of the portfolio as $V_i = V(0) + \sum_{i+\delta t}^{i} \Delta V_i = G_i$, that is the sum of all the portfolio gains plus the initial value (that can also be seen as an initial gain). To

obtain a self-finance strategy, so no cash needs to be added, we must ensure the following condition:

$$V_i = \rho_{i-\delta t} S_i + \gamma_{i-\delta t} C_i + \beta_{i-\delta t} B_i = \rho_i S_i + \gamma_i C_i + \beta_i B_i. \tag{49}$$

Remember that $\Delta V_i = \Delta G_i$ and $V_i = G_i$ we can express both processes using the same numeraire we used for the assets $\frac{V}{B} = V^B$, $\frac{G}{B} = G^B$. We can now define the discounted gain one step ahead:

$$\begin{aligned} \Delta G^B_{i+\delta t} &= G^B_{i+\delta t} - G^B_i = \frac{V_{i+\delta t}}{B_{i+\delta t}} - \frac{V_i}{B_i} \\ &= \rho\left(\frac{S_{i+\delta t}}{B_{i+\delta t}} - \frac{S_i}{B_i}\right) + \gamma\left(\frac{C_{i+\delta t}}{B_{i+\delta t}} - \frac{C_i}{B_i}\right) + \beta\left(\frac{B_{i+\delta t}}{B_{i+\delta t}} - \frac{B_i}{B_i}\right) \\ &= \rho_i \Delta S^B_{i+\delta t} + \gamma_i \Delta C^B_{i+\delta t} \end{aligned} \tag{50}$$

where $S^B = \omega$. This derivation shows that the discounted gain is just the sum of the discounted option and stock; the bond intuitively does not enter into the computation. Continuing with the explanation in Zumbach (2013), the history of the assets is included in the filtration $\mathbb{F}$, but the same is valid even for the weights. Let us take the expectation of the discounted gain change

$$E_i[\Delta G^B_{i+\delta t}] = E_i[\Delta C^B_{i+\delta t}] + E_i[\Delta S^B_{i+\delta t}] \tag{51}$$

where both C^B and S^B are martingales. Given that S^B and C^B are martingales, $E_i[\Delta S^B_{i+\delta t}] = 0$ and $E_i[\Delta C^B_{i+\delta t}] = 0$ so we can conclude that $E_i[\Delta G^B_{i+\delta t}] = 0$. We have shown that G^B and the portfolio value (V^B) are martingales, so the definition $V^B_i = E^{\mathbb{Q}}_i[V^B_n]$ must be valid. The fundamental idea is understanding if the martingale conditions could align with arbitrage strategies. That is not possible, considering that arbitrage exists if $V^B_0 < 0$ and at the same time $V^B_n \geq 0$, which is an evident contradiction with the Martingale condition.

Concluding, if martingales are used to construct a portfolio, the resulting portfolio will also be a martingale. Moreover, the option's price follows a martingale process, as it is based on expected values. This result is relatively easy and general, making this option price formulation valid for a long list of processes.

2.7.2 Monte Carlo pricing scheme

Having delved deeply into the theoretical framework of option pricing, we now transition to its practical implementation into the Monte Carlo simulation methodology. After the simulations of N different paths for the underlying process till the time T, the price of the call can be calculated as

$$C_0 = E^{\mathbb{P}}\left[C_n(S_n)\frac{B_0}{B_n}\frac{d\mathbb{P}}{d\mathbb{Q}}\middle|\mathbb{F}_0\right] \;=\; \frac{1}{N}\sum_{\alpha}\left.\frac{d\mathbb{P}}{d\mathbb{Q}}\right|_{\alpha} C_n(S_{\alpha,n})\frac{B_0}{B_n} \tag{52}$$

where the time t_0 is the time at which the simulations start. The suffix α identifies the single path simulated accordingly with the ARCH process.

2.8 American Option pricing

Pricing American options is more challenging than European ones because of the added exercise flexibility. The early exercise feature of American options transforms their pricing into an optimal stopping problem, and at each time step before maturity, the convenience of exercising must be asses. The value of the early exercise must be quantified, which is why American Options are more valuable and have a higher price. Monte Carlo methods are naturally suited for path-dependent pricing, and several approaches were developed to estimate the option price efficiently. To consistently estimate the price of an American option, we have to integrate and expand the model presented till now. The Zumbach model does not specify any method with this scope, so we decided to extend the model.

The approach we presented in the previous sections can be accommodated because the primary conditions for American option pricing are already in the model. More specifically, we can simulate the different paths using the Garch-based approach explained before. This method gives us a realistic underlying distribution as we did for European ones. Since the change of measure from $\mathbb{P}$ to $\mathbb{Q}$ is analytical, no problems arise when we want to calculate it before maturity. Thus, the change of probability measure must happen at each time step and not just at the ends. We can generalize the Radon-Nikodym formula as follows:

$$\frac{d\mathbb{Q}}{d\mathbb{P}}(i) \simeq 1 - \tilde{R}_i + \frac{\tilde{R}_i^2}{2} + \frac{\tilde{y}_i}{2} - \frac{\tilde{\sigma}_{int,i}^2}{2} \tag{53}$$

with $t_0 < i < T$. Thanks to the analytical estimation of $\frac{d\mathbb{Q}}{d\mathbb{P}}$, the model is very flexible, and we have no problems calculating the derivative at different time steps. Therefore, we have a ready-to-use set-up with a path simulation process and a change of probability measure. Lastly, we must assess a rule to understand whether the early exercise is convenient. In this context, the Least Square Montecarlo (LSM) is an optimal approach.

The LSM method proposed by Longstaff and Schwartz (2001) is an ideal solution for our pricing problem. The model is sufficiently elastic to adapt our framework without any further assumptions; furthermore, the calculations are pretty simple and do not require outstanding computational power. In addition to that, the LSM model can be used even to price complex derivatives over the classical vanilla options. As we introduced before, the crucial aspect in pricing American options is considering that at each time, the investor compares the option's current value with the expected future one. For this reason, the model basis is the construction of a rule determining the optimal exercise. The basic idea of setting such a rule is to evaluate the conditional expectation of the future payoff given the current one by a cross-sectional linear regression between the two. The cross-sectional component arises between the different trajectories of the simulation. Thus, the payoff of

the continuation from each path is regressed on functions of the state variables, and the fitted values provide an estimate to obtain the conditional expectation function. Since the pricing is obtained as an expectation over the risk-neutral measure, the price processes used in the original paper were also risk-neutral. In particular, a classic Brownian motion with a risk-free drift growth or a Merton jump-diffusion process, both with constant volatility. We already explained in the first chapter that such models poorly represent the actual underlying behaviors. For this reason, the realistic ARCH approach with a stock price process in the $\mathbb{P}$ proposed can augment the LSM model. Specularly, the LSM is a very effective tool to augment the Zumbach model and be able to price American options. The two models can be consistently merged, and both approaches would benefit from that.

To be more specific, we have an underlying process in the probability space $(\Omega, \mathbb{F}, \mathbb{P})$, we already know that from such space, we can define an equivalent martingale measure (EMM) $\mathbb{Q}$. The time horizon for the pricing is the same as for the European options $[t_0, T]$, and along this time, we have N different trajectories. Each possible pathway can be represented as a general draw α from our state space Ω. The cash-flow path for the option must be evaluated at each time t_i, and it is denoted as $C(S_\alpha, t_i; t_k,\ T)$, $t_k < t_i < T$. It is worth mentioning that the American options can usually be exercised in the continuum time during the trading day, although time series samples are usually daily. For this reason, we can only approximate the option's value, and this approximation would be better by increasing the time step for the valuation $T/\delta t = n$. The algorithm scheme is intuitive: starting from the end of each path, we calculate recursively the continuation value and compare it with the current one. The continuation value, in our environment, can be defined as follows:

$$F_{k,\alpha} = E^{\mathbb{P}}\left[\sum_{i=k+1}^{T} \left.\frac{d\mathbb{Q}}{d\mathbb{P}}\right|_{\alpha,i} C(S_{\alpha,t_i,}, t_i; t_k, T)\ \ \frac{B_i}{B_n} \,\middle|\, \mathbb{F}_k \right] \tag{54}$$

Remember that options can be exercised only once, so when the continuation value is lower than the current one, we eliminate any future possible payoff because the correct choice is to pay the strike immediately. The paper by Longstaff and Schwartz (2001) found a way to approximate analytically this expectation through a simple linear regression. For the basis function set, we chose the family of Laguerre and Chebyshev polynomials of the first kind. Like orthogonal polynomial systems such as Hermite or Legendre polynomials, Laguerre ones can approximate certain functions in numerical methods. Their orthogonality properties can improve the model by reducing computational errors and improving numerical stability.

The Laguerre polynomial[17] is given by:

$$L_0(X) = \exp(-X/2), \tag{55a}$$
$$L_1(X) = \exp(-X/2)(1 - X), \tag{55b}$$
$$L_2(X) = \exp(-X/2)(1 - 2X + X^2/2), \tag{55c}$$
$$L_n(X) = \exp(-X/2)\frac{e^X}{n!}\frac{d^n}{dX^n}(X^n e^{-x}), \tag{55d}$$

On the other hand, Chebyshev polynomials[18] of the first kind are $T_n(x) = n\cos(\arccos(x))$ and must satisfy the recurrence relation:

$$T_0(x) = 1,\ T_1(x) = x,\ T_n(x) = 2XT_{n-1}(x) - T_{n-2}(x) \tag{56}$$

When there is no closed-form solution or (in our case) it is computationally expensive, we can use Chebyshev polynomials to approximate option pricing functions. Due to their orthogonality and unique properties, they can offer faster convergence and better accuracy than standard polynomial approximations. Both solutions return solid and stable results, but the difference is in the time to compute the polynomials.

We have established the sets of basis functions, and it is now possible to perform the conditional expectation according to them. Given that the price of the call was reduced simply to:

$$C_0 = \frac{1}{N}\sum_{\alpha}\max(F_{\alpha,i}, C_{\alpha,i}), \tag{57}$$

where i goes from maturity T till t_{0+1} recursively. We obtain our American Option Pricing Model by calculating the max between the continuation value and the current payoff at each time step and then averaging for each trajectory.

[17]Figure 23
[18]Figure 24

3 Applied Model

In this chapter, we will explore the results of the model explained till now. The focus will initially be on the set-up phase, in which we will estimate the parameters and all the essential components for the option pricing. Later, we will delve into the price series, comparing the different types of options (Call, put, European and American). To conclude, we will focus on the implied volatility by choosing two different time frames and trying to draw out important information on the market.

3.0.1 Model Set-Up

The following section examines the model applied to the SP500 index, and the time frame chosen is the same one used by Zumbach and Fernández (2013). This way, we can compare the results better and verify the parameters suggested in the paper. The time series used are three: the SP500 price series[19] (Bloomberg), the dividend yield q (Refinitiv), and the risk-rate[20] r_{rf} (Kenneth et al. - Data Library)[21]. The period under consideration goes from january 1996 to june 2010.

The first step was calculating the relative returns over increasing time horizons ΔT (Figure 22), and we described how to calculate them in Equation 10. The time horizons are estimated accordingly with Equation 19a. The parameters chosen are $\rho = 2$, $\Delta T_1 = 1$, $\tau_1 = 5$, and $\tau_0 = 520$ which return

ΔT	1	2	4	8	16	32	64	128	256	512
τ	5	10	20	40	80	160	320	640	1280	2560

As we already explained, in this way, it is possible to capture the different characteristics of the returns over increasing time intervals ΔT.

The second crucial step in our model is the GARCH estimation, and following the methodology of Zumbach et al. (2014) explained in the section 2.2.3, we were able to estimate the following parameters:

Θ	w_∞	σ_∞	λ_{lev}	λ_{range}	ν
Value	0.05	0.20	0.9	0.25	7

Table 1: Garch parameters

The estimated parameters are consistent with the original paper and mirror the expected characteristics of the SP500 index. The long-term volatility σ_∞ is set to the empirical mean observed in the market and determine a notable baseline volatility.The value of w_∞ suggests that 5% of the effective volatility is attributed to long-term, and such a low value indicates

[19] Figure 21
[20] Figure 27
[21] *https : //mba.tuck.dartmouth.edu/pages/faculty/ken.french/data_library.html*

that the specific model components already capture most of the volatility. Furthermore, the model highlights a strong leverage effect, as evidenced by the value of λ_{lev}, which is almost at the maximum value possible (1).[22]

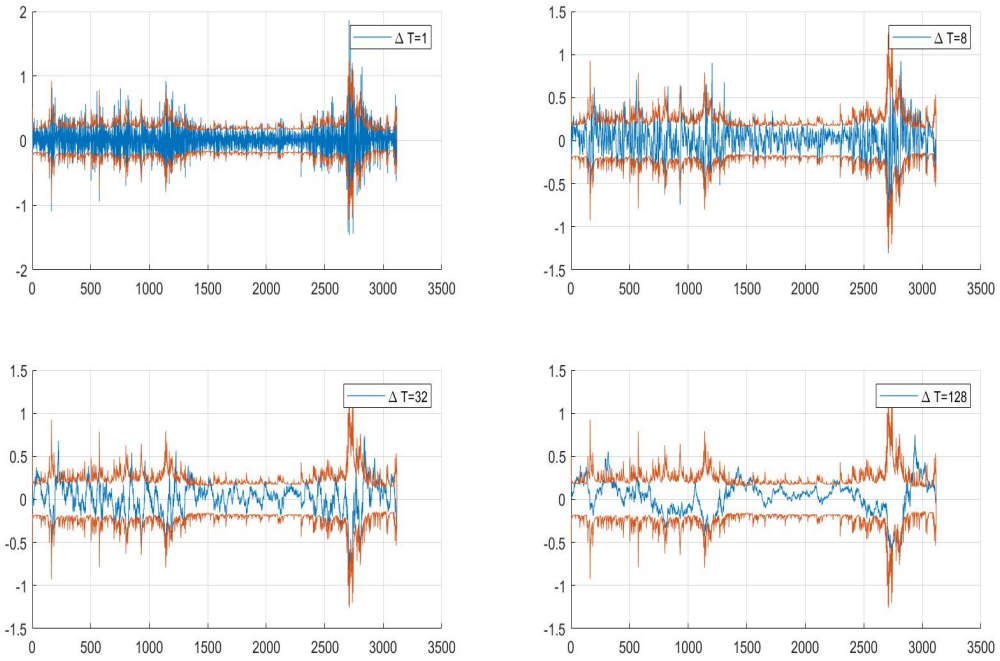

Figure 7: *Effective variance calculated with the leveraged multiscale ARCH, plotted with the returns at different scale.*

The daily volatility ranges between 10% and 65%, where the peak is during the 2008 Financial crisis. Once we have estimated the underlying process parameters, we can perform the Monte Carlo simulations. The structure of the recursive Monte Carlo process is:

- We started generating a random t-distributed matrix with the row length corresponding to the number of time steps to maturity(n). The width depends on the number of simulations (N) divided by the antithetic scheme:

$$\begin{matrix} z(1,1) & z(1,2) & \cdots & z(1,N/2) & -z(1,1) & -z(1,2) & \cdots & -z(1,N/2) \\ z(2,1) & z(2,2) & \cdots & z(2,N/2) & -z(2,1) & -z(2,2) & \cdots & -z(2,N/2) \\ \vdots & \vdots & \ddots & \vdots & \vdots & \vdots & \ddots & \vdots \\ z(n,1) & z(n,2) & \cdots & z(n,N/2) & -z(n,1) & -z(n,2) & \cdots & -z(n,N/2) \end{matrix}$$

  The preallocation of the matrix speeds up the computational time.

[22]The impact of the leverage effect on the simulation can be seen graphically in Figure 25

- The next step is initializing the returns tensor, with n rows and N columns repeated for each k time horizon.

$$\begin{bmatrix} r(1,1,k) & r(1,2,k) & \cdots & r(1,N,k) \\ r(2,1,k) & r(2,2,k) & \cdots & r(2,N,k) \\ \vdots & \vdots & \ddots & \vdots \\ r(n,1,k) & r(n,2,k) & \cdots & r(n,N,k) \end{bmatrix}$$

  Each k matrix inside the tensor contains the returns at different time horizons.

- The returns are calculated with Equation 12a, and right after the prices with Equation 12b. Using the just computed prices, we can retrieve the returns at different time scales using Equation 10. It is now possible to estimate the effective variance σ_{eff} and use it to calculate the new returns. We completed the simulation by repeating this step until maturity T.

The heteroscedastic feature of the variance combined with a high leverage effect results in very different paths compared with the classic stochastic processes used to simulate underlying. Unlike standard methodologies that rely on a constant volatility assumption (like the geometric Brownian motion), our realistic features result in asymmetric distributions, stock crashes, and highly positive outliers. The broader dispersion of our Monte Carlo paths, especially during turbulent times, captures the fat-tailed stylized fact, where extreme events are more probable to be predicted than a standard normal distribution. Our realistic simulation, which more accurately represents extreme market movements, results in theoretically reasonable and practically robust option prices. After the simulations, we can now calculate R, σ_{int}, and y (Equation 38), and if the δt expansion is correctly specified, we can use it to approximate the final prices. Thus, we can use Equation 39 to test this approximation together with the simplest $S_n \simeq F_n \exp(R)$. Using a simple RMSE, we can evaluate the two estimates, and this assessment indicates that both approximations are robust and consistent. The distributions and the plots for the just estimated elements are in Figure 26.

The option pricing could not be performed without estimating the Radon-Nikodym derivative, and to do it, we need first to find the drift μ, risk-premium ϕ, and the market price of risk λ. The formulas used are Equations 32a and 32b, but we must be careful with the annualization or the time scale. As reported in Zumbach and Fernández (2013), the process parameters are optimized using a business day count of 1 $year = 260$ $days$ while most providers give the risk-free rate and the dividend yield on a 365 $days$ base. The problem can be solved easily by the relation $r^*_{rf} = \frac{7}{5} r_{rf}$ where r^*_{rf} is the new risk-free we must use, and the same relation is valid for dividend yield q. To estimate the drift, we must compute the forecast accordingly with Equation 23a and 23b. The parameters in Table 1 give a robust estimation of the volatility with an RMSE stable around 0.12. In

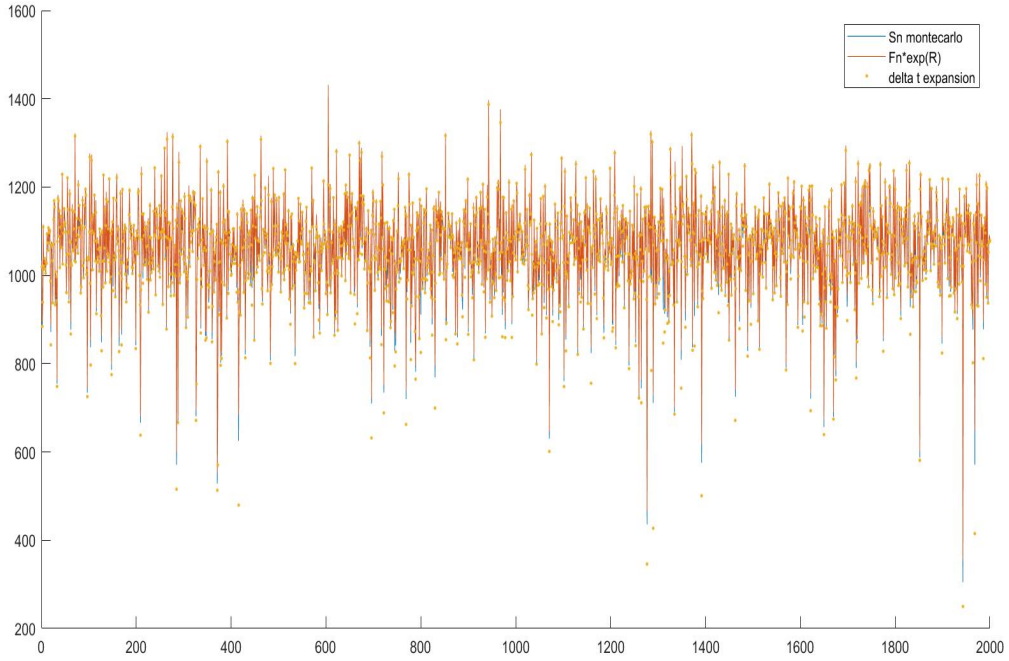

Figure 8: *The final prices S_n from the Monte Carlo compared with the two approximations $F_n \exp(R)$, and $F_n\left(1 + R + \frac{R^2}{2} + \sum_i(\mu_i - r_{rf}) - \frac{y}{2} - \frac{\sigma_{int}^2}{2}\right)$*

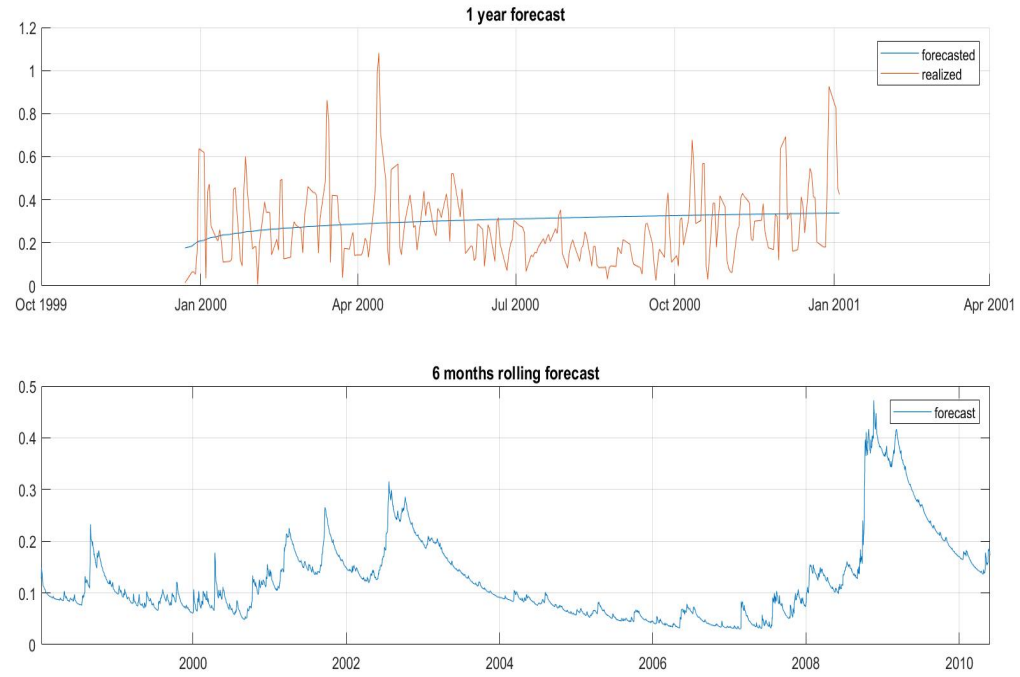

Figure 9: *Top figure: 1 year forecast estimation. Bottom figure: 6 months rolling estimation, used to calculate μ.*

Figure 9, we can see two different uses of the forecast: in the up section, a classic GARCH forecast for one year where the volatility consistently converges, and in the bottom section, the day-by-day six-month forecast. The second one is precisely $\tilde{\sigma}$, that is the forecast we need to calculate μ[23] as described in Equation 27. The drift μ is defined as a convex relationship with the volatility, and the parameter σ_{rp} sets the convexity. The parameters are set to $\sigma_{rp} = 0.17$ and $\beta = 0.075$ to match the empirical evidence about the drift and the risk-premium. This way, the mean drift is of order 6%, and the mean risk premium is around 2.

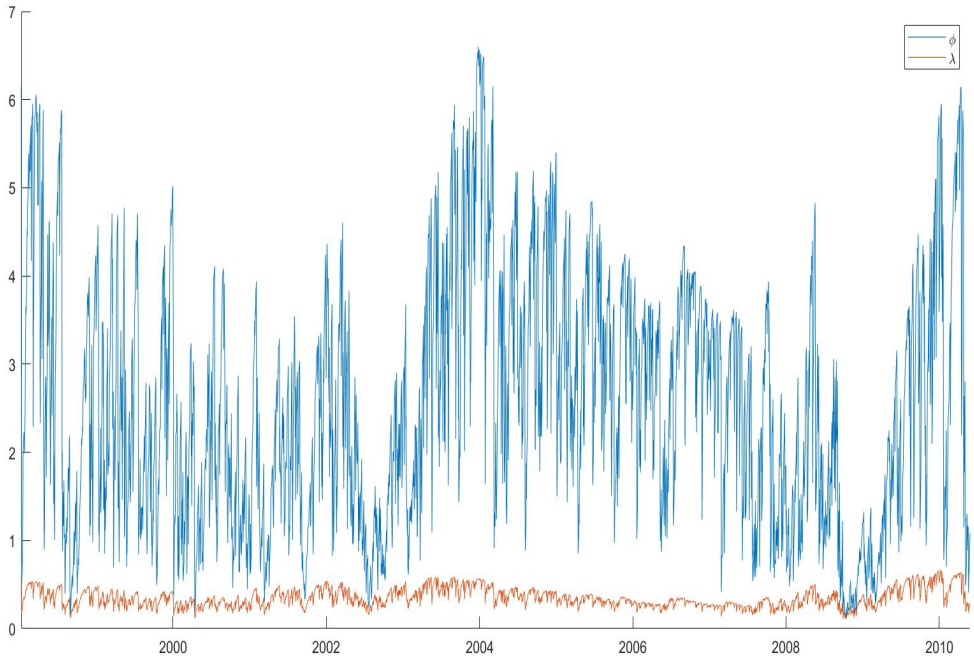

Figure 10: *Market price of risk λ and risk premium ϕ*

Calculating the Radon-Nikodym derivative using the just estimated elements is now possible. Moreover, we can calculate the options price since all the preliminary steps are completed. For European options, the derivative is computed at each maturity and multiplied by the price S_n for every trajectory. The price probability distributions change more in the longest time to maturity; thus, the change of probability measure is less influential for short horizons. Similarly, for underlying processes with higher variances, the change in measure can introduce notable variations in the modeled price dynamics. When computing the change from $\mathbb{P}$ to $\mathbb{Q}$, a noteworthy observation is the resultant shift in the price density function of the underlying process. As shown in Figure 11, the Rason-Nikodym derivative $\frac{d\mathbb{Q}}{d\mathbb{P}}$ shifts the density to the left, and this happens because moving to the risk-neutral essential means removing the drift of the process and substituting it with the risk-free rate.

[23]Figure 27

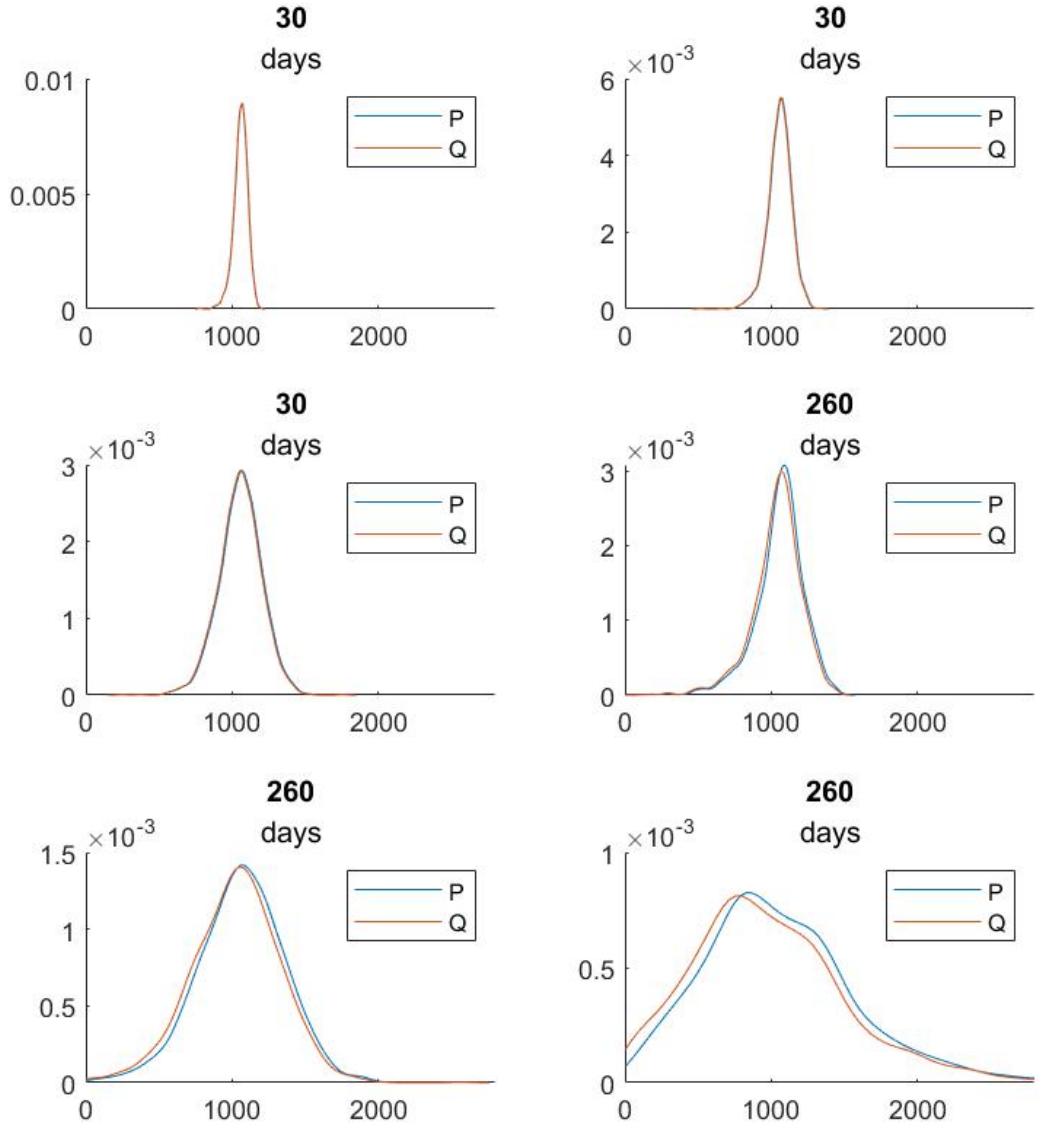

Figure 11: *The different probability density functions for the final prices S_n in $\mathbb{P}$ and $\mathbb{Q}$ measures. Plotted at increasing $\sigma_\infty = 0.1, 0.2, 0.4$. Two different time horizons: 30 days and 260 days.*

In the American option context, the idea is pretty much the same, and the only difference is that we must replicate the calculation of the derivate at each time step.

3.0.2 Option Pricing results

The European option pricing is now straightforward, and all that remains is to compute the payoff functions, apply the derivative, and discount at the risk-free rate. While the consistency of this method was widely tested in the original papers, we must test with

the American option framework adapted to this context. We experimented using the two basis functions mentioned in the previous chapter(2.8): the Laguerre and Chebyshev polynomials. While both sets of basis functions could capture the critical features of our data effectively, we observed that their result prices were markedly similar. For this reason, using both approximations was unnecessary, redundant, and computationally intensive. The computation time, especially for large datasets, would grow substantially using both bases. We deeply tested the Laguerre base and, in general, the entire model. We found them particularly efficacious in delivering robust estimations with consistently low standard errors observed in the results. This precision highlights the model's reliability and ability to provide stable outcomes, even under varied data scenarios. Furthermore, as already noticed by Longstaff and Schwartz (2001), the simple choice of X, X^2, X^3 as the basis function gives almost identical results compared with the Laguerre polynomials up to third order. Thanks to this finding, we can enormously reduce the computational time without losing precision, highlighting the process's robustness to the choice of the basis function.

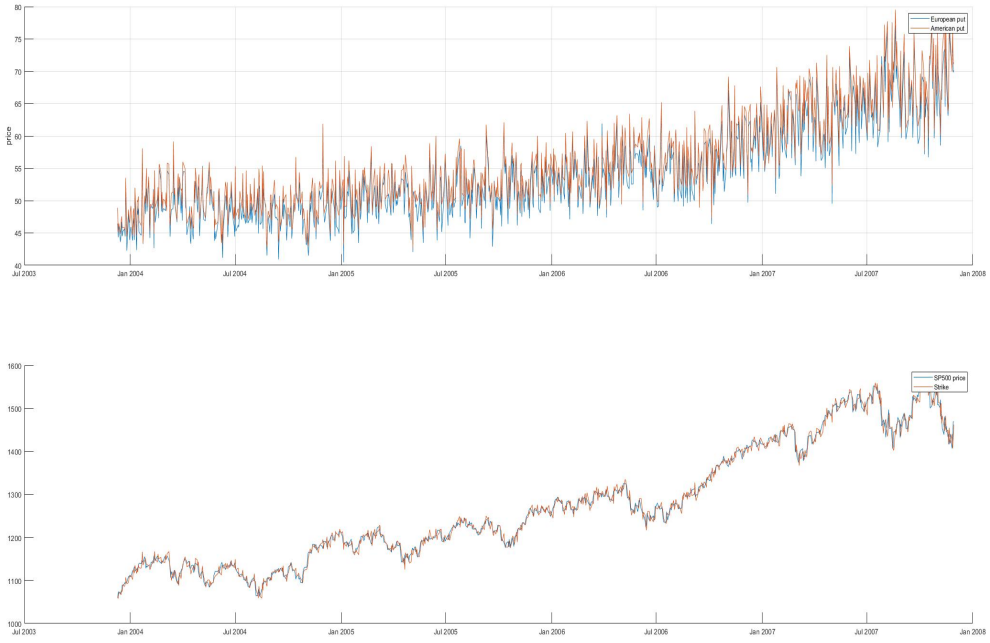

Figure 12: *American and European put option prices compared. Maturity 30 days*

As expected, there is the presence of a premium associated with the early exercise feature of American options. That is why the American put option prices are consistently above their European counterparts, more significantly as maturities extend. Extending the timeframe introduces more potential scenarios where market conditions favor early exercise. The longer the maturity, the greater the window of opportunity for an optimal exercise moment,

maximizing the investor profit potential.[24] Figure 13 shows the European and American option prices in function of time and strike. As expected, the American option price surface lies above the European one, with only a few sections where the surfaces intersect.

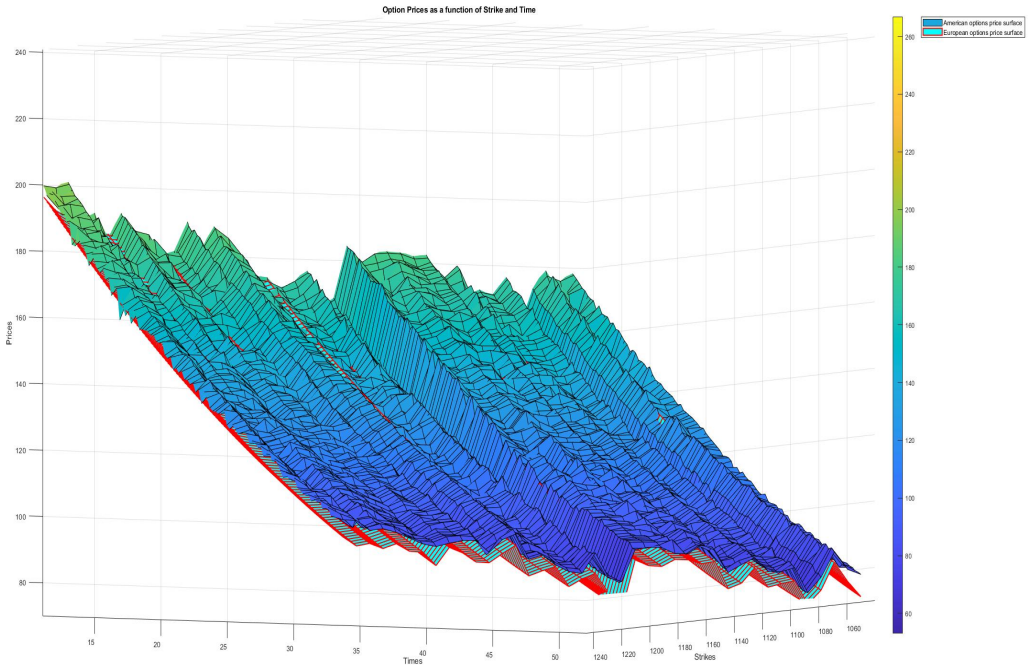

Figure 13: *American and European put options price surfaces. Maturity 1 year*

In our analysis of the American option estimation, we want to underlie the relationship between the number of simulations and the resultant standard errors from the associated linear regressions. In particular, the standard error is calculated as $\sigma_Y/\sqrt{N}$ where Y are the final discounted payoffs. An evident inverse relation exists between the number of simulations and standard errors. However, what is particularly encouraging is the rapid convergence of prices, even with a relatively low number of simulations. For example, with $N = 2000$, the option prices were already stable. While escalating the simulations to the range of 40,000 fine-tuned the standard errors, making them lower and more precise, it had little influence on the estimated option prices. These prices remained relatively unchanged, highlighting the model's efficiency. As we can observe from Figure 14, the standard errors are positively related to the time to maturity. However, this is an expected result since increasing the horizon means increasing the early exercise opportunities and price dispersion.

[24]Figure 30 highlights the difference in the American options premium at increasing time horizons.

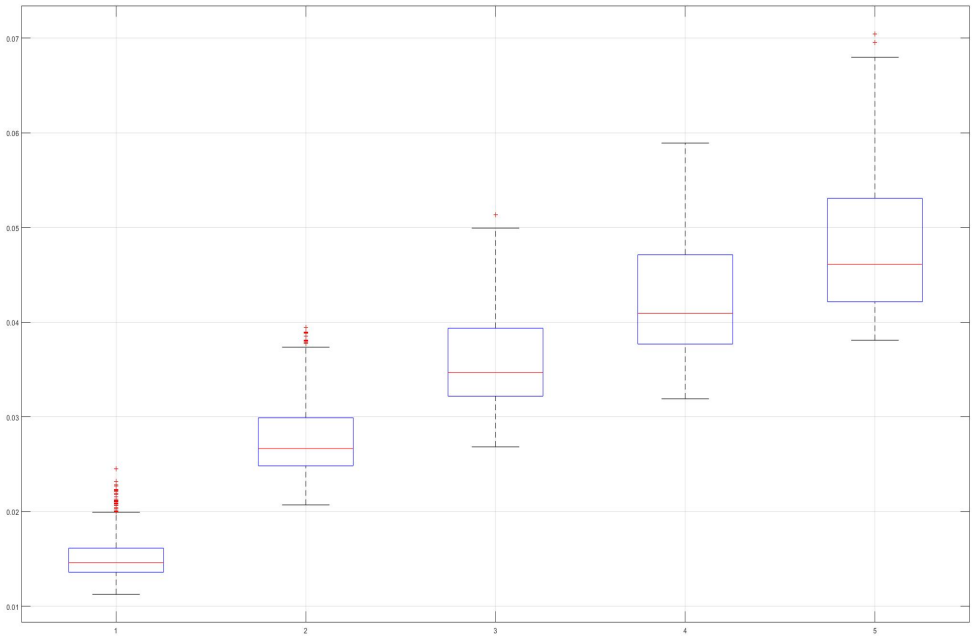

Figure 14: *Standard error boxplots for increasing time to maturity: n=30,90,150,210,270 (days). N=40000 (simulations)*

3.0.3 Implied Volatility

Another essential aspect we must delve into before concluding is the volatility implied by the estimated option prices. This fundamental metric might give us essential insights into the underlying process and investors' expectations. As we mentioned in section 1.1.1, the BSM model can be used to estimate the process volatility implied by the computed prices. The shape of the implied volatility surface can drastically change over time because numerous factors influence it. We experiment with this characteristic by estimating our American put options' implied volatility in two financial and market contexts. The first one is from January 2004, which was, for the SP500, a bullish period with a relatively stable variance. As opposed, the second frame chosen is in the middle of the 2008 financial crisis during the fall of the stock market.

Figures 15 and 16 are the volatility surfaces for the above time-frames, and we can notice quite diverse structures between the two. Firstly, it is significant to notice that both surfaces present an accentuated smile, which can be observed better in Figure 17. The smile and its asymmetry directly result from the leverage incorporated into the underlying process. Furthermore, the smile has a decreasing path over time as it should be from the economic intuition; however, it is persistent till 520 days, the maximum number of days incorporated from our long memory ARCH process. This finding confirms the model's ability to capture diverse effects at increasing time horizons.

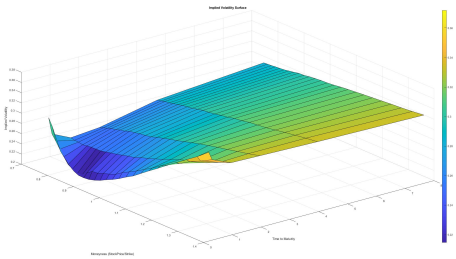

Figure 15: *Implied volatility surface for January 2004 American put options*

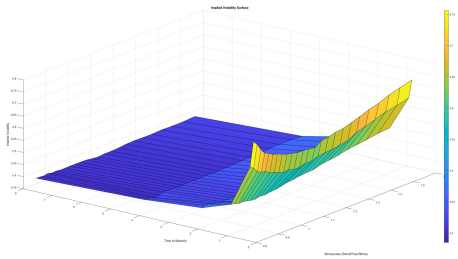

Figure 16: *Implied volatility surface for October 2008 American put options*

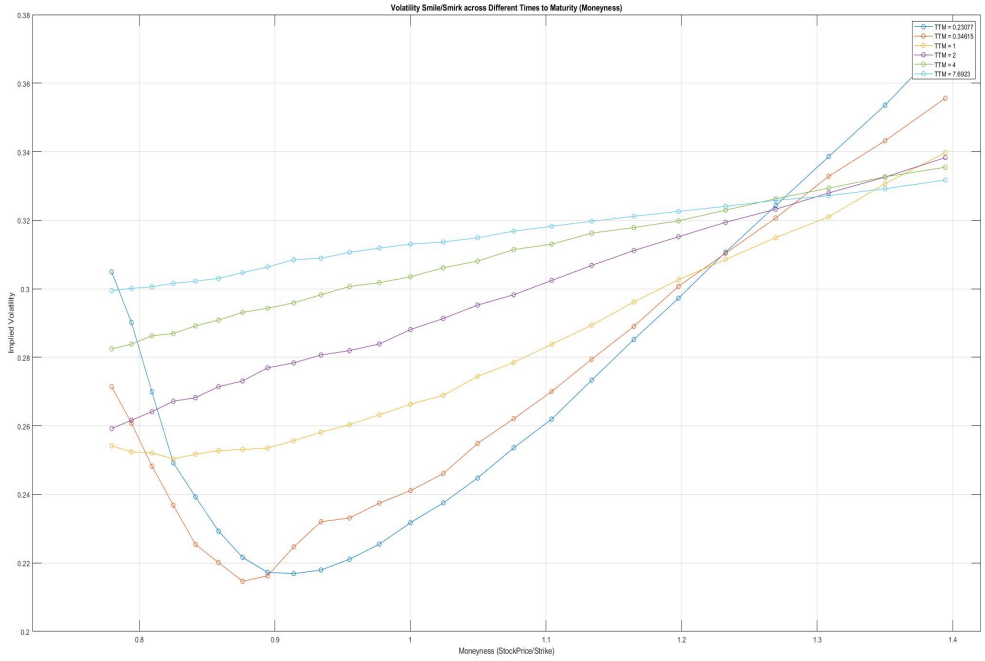

Figure 17: *Volatility smile for January 2004 American put options. Calculated at different time horizons.*

In contrast with the BSM, the process captures the negative skewness and the leptokurtic distribution stylized facts, reflecting such properties on the implied volatility surface. According to the excess kurtosis, large draws are more likely to happen than expected under Gaussian distribution. As a consequence, deep OTM and ITM options are more likely to be bought, increasing their prices. Using the BSM option pricing model to map the implied volatility means higher prices are associated with higher volatilities, enhancing the smile.[25]The Same argument can be used for the negative skewness, which steepens the ITM put side or OUT call side.

The second component of the IV surface is the term structure, and from figure 18 and

[25]Sinclair (2010)

19, we can compare the 2004 and 2008 ones. The shape of this curve provides insights into the market's expectations about future stock price volatility. The Figures show the backbone, the term structure for at-the-money options, and two directions for far OTM and ITM options.

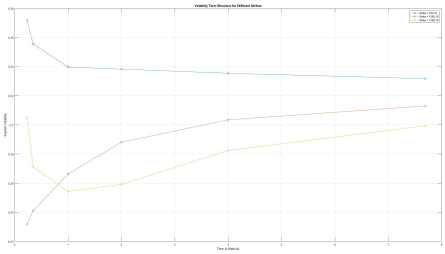

Figure 18: *Term structure for January 2004 American put options*

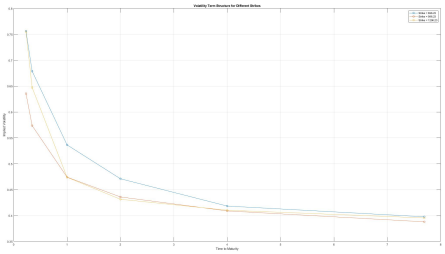

Figure 19: *Term structure for October 2008 American put options*

In 2004, we had a general upward trend curve for the term structure, with the only exclusion of the highly out or in-the-money strikes. An upward-sloping term structure suggests that the market expectations are directed towards a higher future volatility than the short-term. This is common in stable or bullish markets with more certainty in the short term, as in the 2004 market. Conversely, when short-term volatilities are high, the term structure tends to be a decreasing function. For this reason, the notable downward-sloping term structure in 2008 indicates that the market expected higher volatility in the near term compared to the long term. Given the backdrop of the financial crisis, there is uncertainty for the immediate future, with an opinion of future stabilization. Another factor could be that in times of extreme market stress, there is often a rush to buy short-term protective options (like OTM puts) as a hedge against further declines. Doing that can disproportionately drive up the IV for short-term options compared to longer-term options.

Conclusions

The Zumbach model we presented in this thesis can effectively encapsulate the significant financial stylized facts. The ARCH process is regulated by a set of parameters, allowing us to accommodate different financial asset characteristics. Furthermore, we can calibrate the process and accommodate time-evolving underlying features to match market option prices. The American option extension we proposed catches all the benefits of the Zumbach work and extends it efficiently and robustly. The LSM method can perfectly integrate with the Zumbach model and value options consistently and time-savingly. Thanks to this framework, we can compute option prices and explore the dynamic aspects of the market, its drivers, and expectations.

In this thesis, we first explored the theoretical background crucial to fully understanding the presented model and the context in which it lies. In particular, close attention was given to the foundational Black, Scholes, and Merton model. Awareness of the BSM's strengths and weaknesses is essential to understanding the directions the following financial researchers pursued. In the second chapter, we deepened the model, analyzing each aspect and making it reproducible for those who want to engage in this method. The model explanation is intended to illustrate it and give the theoretical background behind each section of the used methodology. In the last chapter, we put into practice the framework explained till then. We first explained how to set the model up and showed the step-by-step results; this way, the reader could better understand all the pieces needed to complete the option pricing puzzle. We concluded the chapter by analyzing and comparing the option prices obtained and constructing the implied volatility surface. We studied the implied volatility behaviors in different market conditions, extrapolating significant insights into the investor's expectations.

The model proposed in this thesis could be used to accomplish several tasks in different financial areas. The first obvious challenge the model helps to solve is derivative pricing per se. However, the model can be extended beyond traditional options to price complex financial derivatives. As we showed, by analyzing the volatility surface (smile, smirk, or term structure) generated by the model, it is possible to obtain insights into market sentiment and participants' views on future volatility. This option pricing framework can have interesting educational utilities and help understand the drivers of the financial markets experimenting with them.

While the model shows promising attributes, it is crucial to acknowledge its limitations. In periods of high volatility and quick market movements, the model captures those changes slowly. An analysis with high-frequency data would result in better estimates for these frenetic periods. Moreover, some market dynamics during crisis periods can only be captured partially. For example, a further model extension might add an options liquidity premium factor. The liquidity premium is often a critical asset characteristic in low liquidity times, and during such periods, the prices can deviate from our model. Market participants

demand this premium as compensation for the increased risk associated with illiquid assets. Especially for short-term protective puts, the price change could be significant, leading to increased implied volatility. However, a notable strength of our model lies in its intrinsic flexibility and adaptability. The model is designed with a modular architecture that allows for future enhancements in an intuitive way. Whether integrating new market dynamics, adding layers of complexity, or adjusting to accommodate new financial instruments, the model's adaptability ensures that it remains relevant and provides precise estimations. Thanks to its intrinsic characteristics, the model can evolve alongside financial market research and innovation.

A Figures

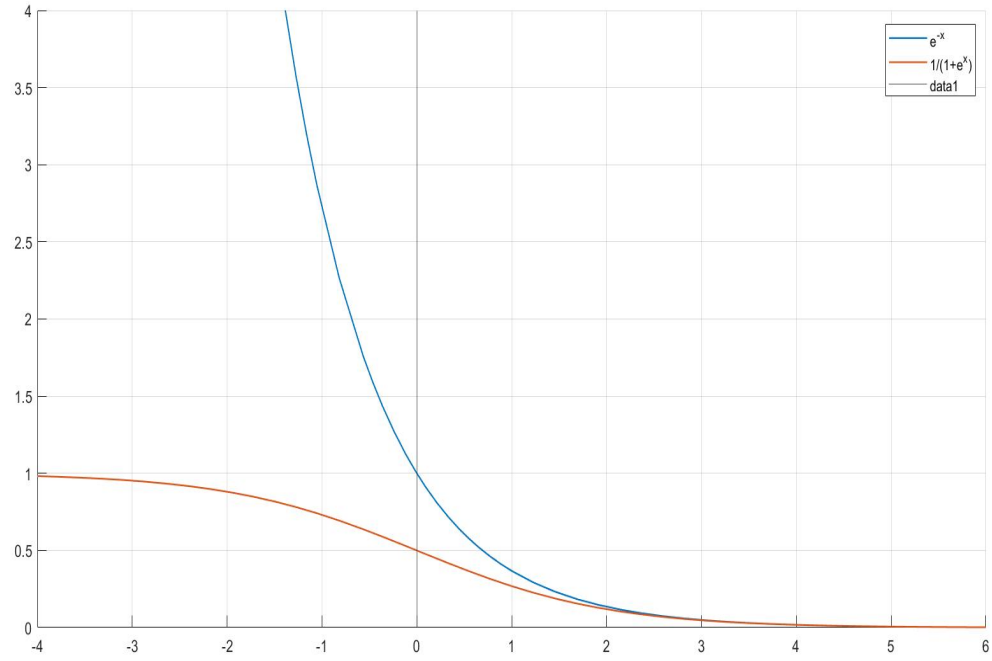

Figure 20: *Comparison between the two risk aversion functions* e^{-x} *and* $\frac{1}{1+e^x}$.

Figure 21: *SP500 historical prices from '02-Jan-1996' to '28-May-2010'. Data source: Bloomberg.*

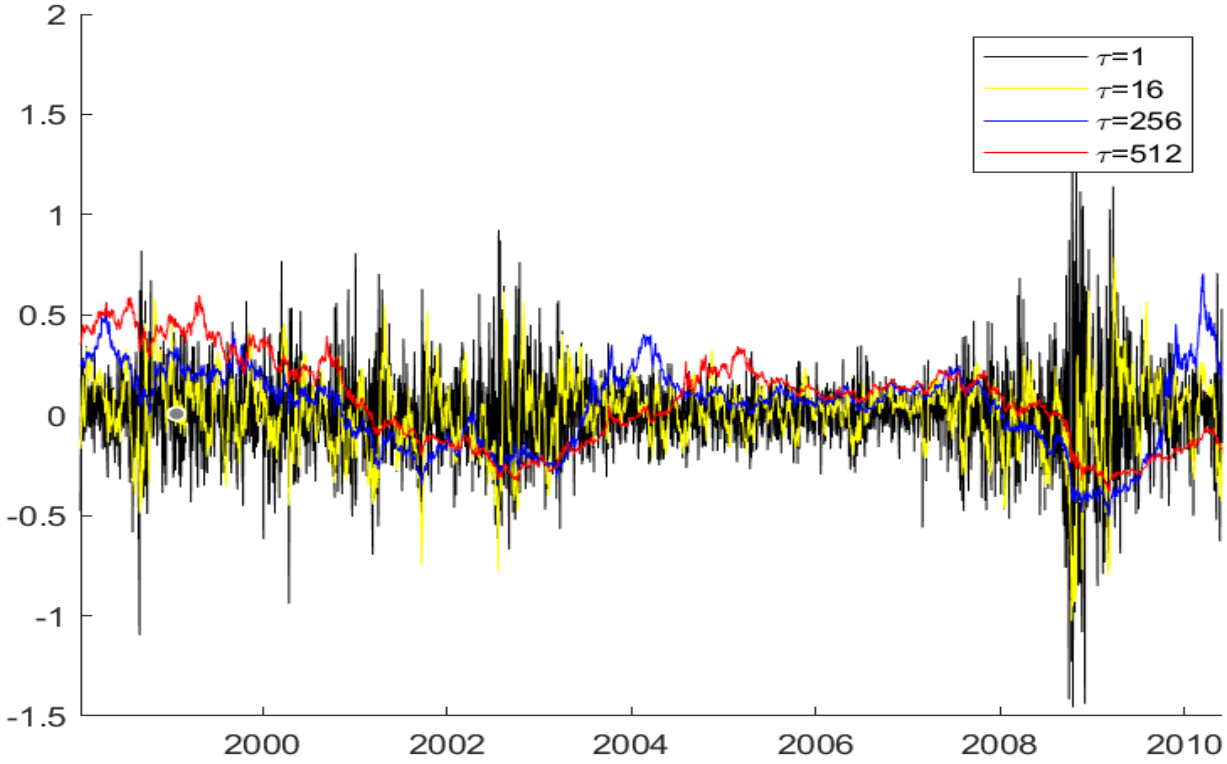

Figure 22: *Relative returns for SP500 at different time horizons* τ

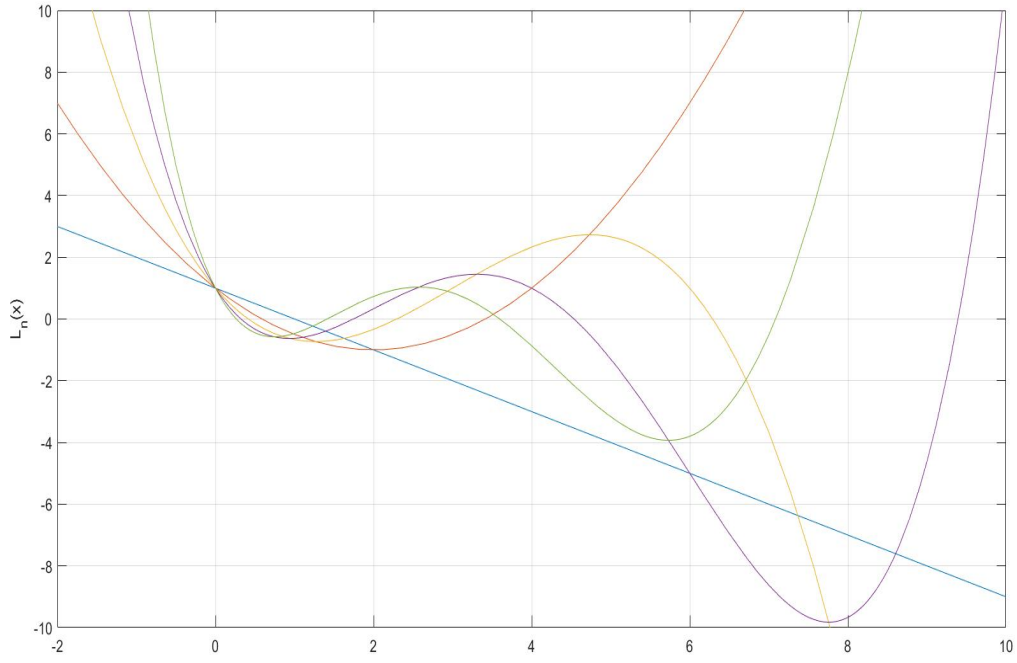

Figure 23: *Laguerre polynomial of order 1 through 5*

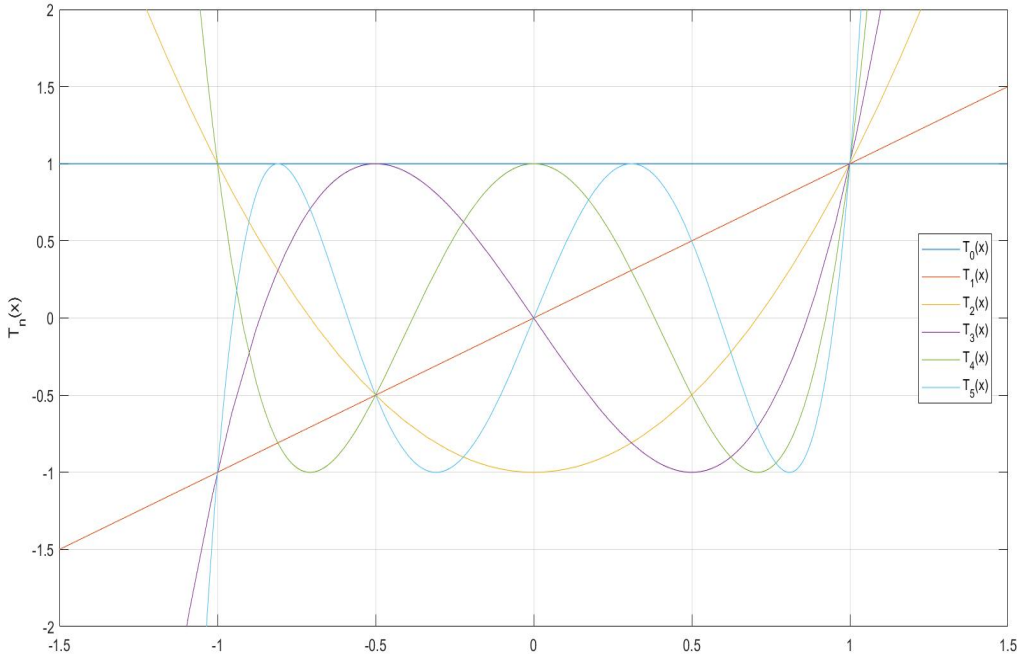

Figure 24: *Chebyshev polynomial of order 1 through 5*

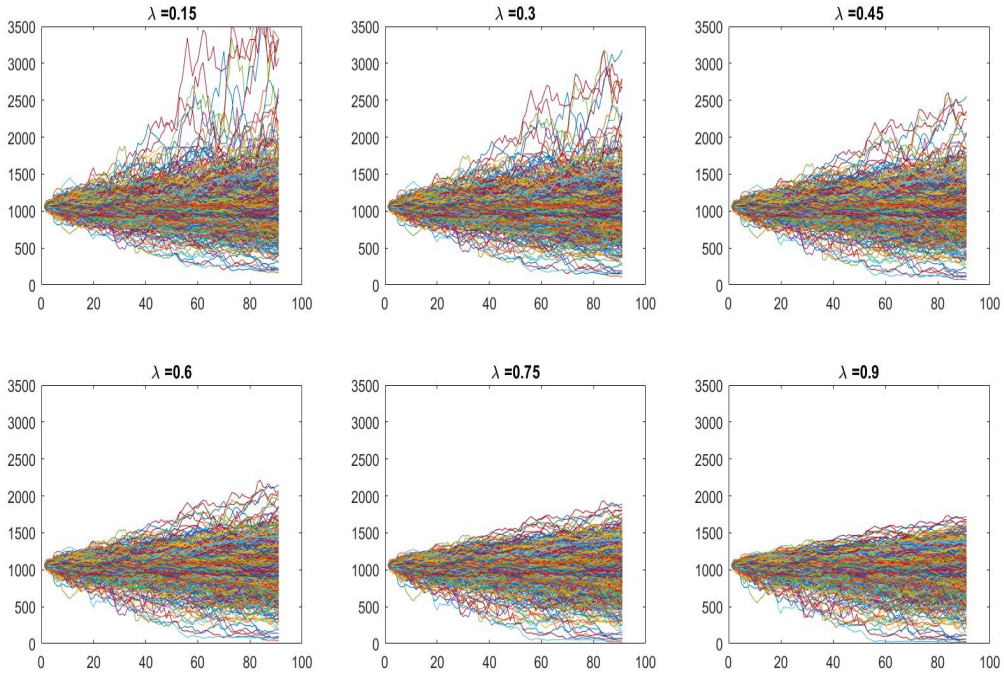

Figure 25: *Impact of the leverage effect λ_{lev} on the simulation, from high left (lower) to bottom right (highest). The number of trajectories $N = 2000$ and the time steps $n = 90$.*

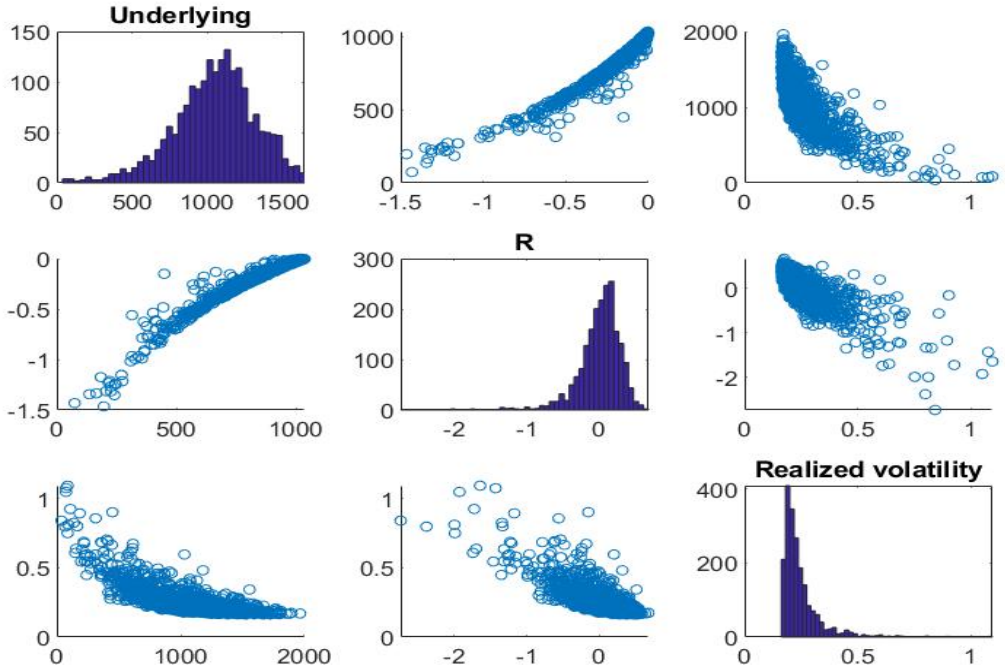

Figure 26: *The distributions and the cross-plot between the final prices S_n elements: S_n, R and σ_{int}.*

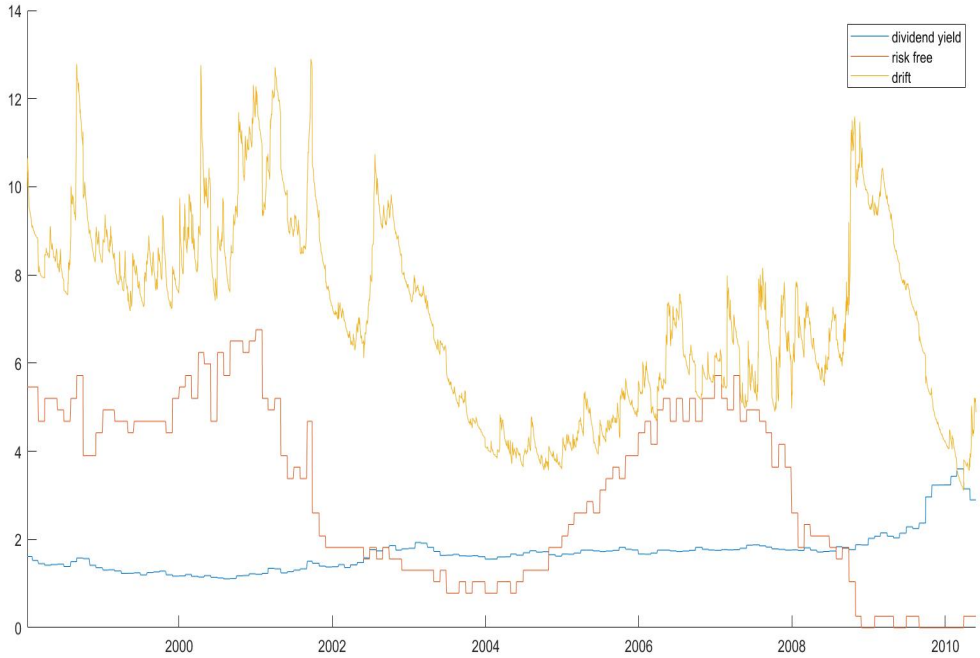

Figure 27: *The drift μ, the dividend yield q, and the risk-free r_{rf} compared. $\beta = 0.075$ and $\sigma_{rp} = 0.12$*

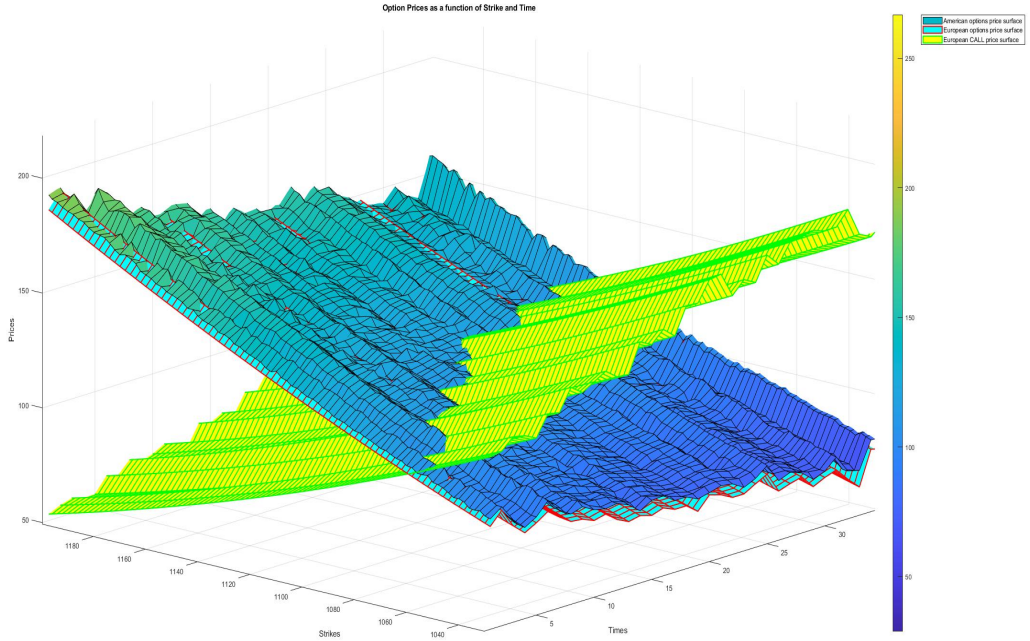

Figure 28: *Price surfaces for European call options, European put options, and American put options. Maturity 1 year*

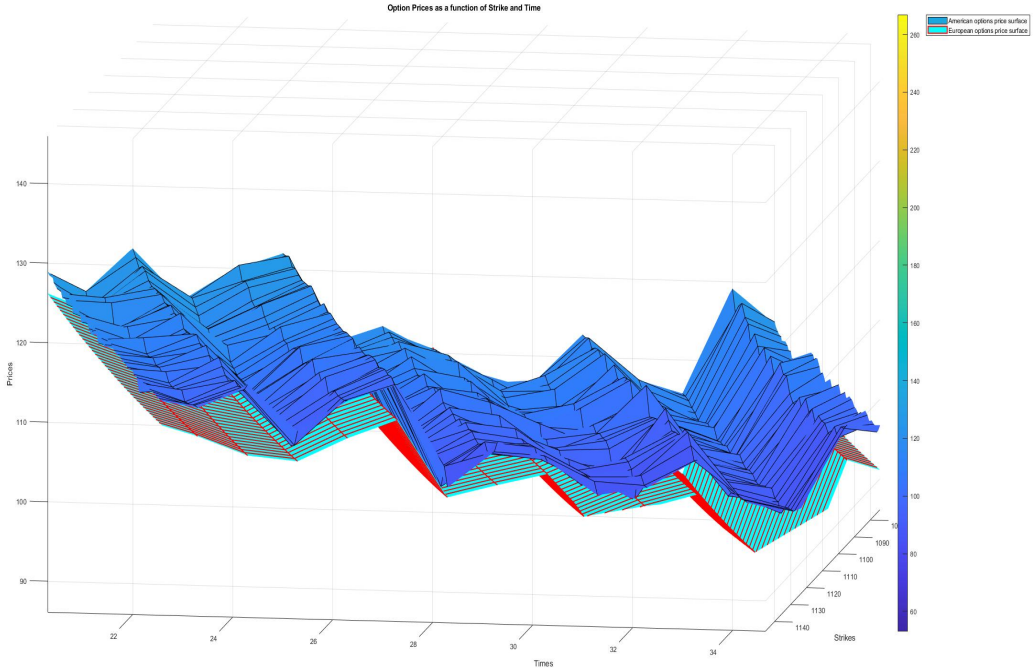

Figure 29: *Close-up between the American and European price surfaces. Maturity 1 year*

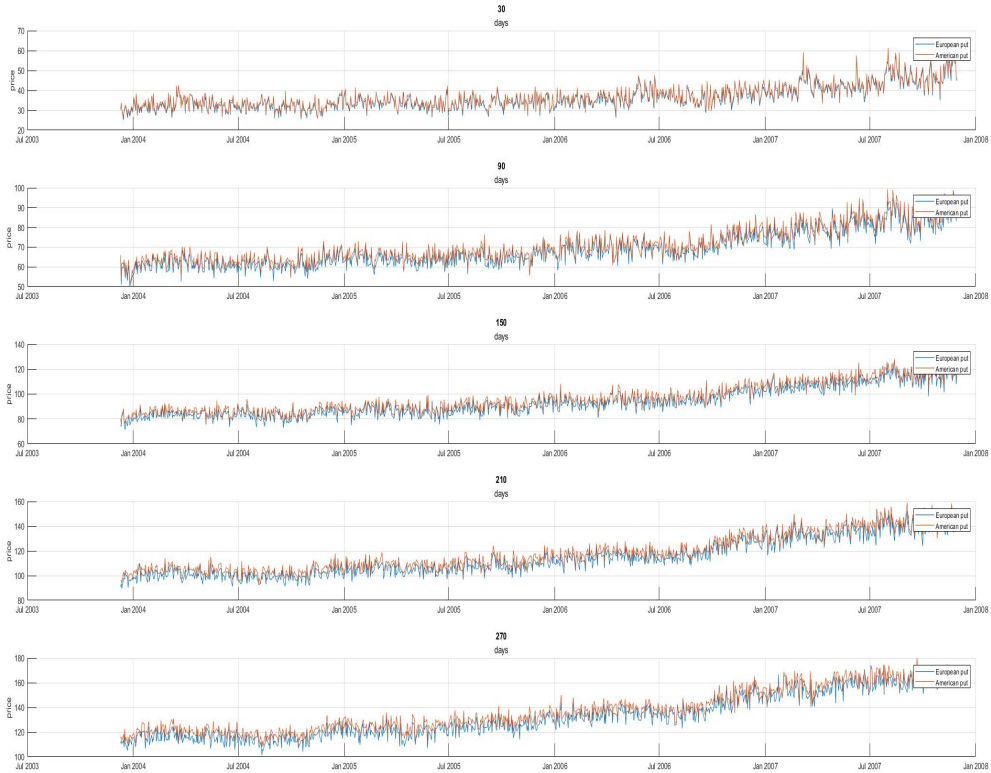

Figure 30: *European and American option prices at increasing maturities.*

References

Barone-Adesi, G., and Whaley, R. E. (1987) Efficient analytic approximation of american option values. *The Journal of Finance*, *42*(2), 301–320. https://doi.org/https://doi.org/10.1111/j.1540-6261.1987.tb02569.x

Black, F., and Scholes, M. (1973) The pricing of options and corporate liabilities. *Journal of Political Economy*, *81*(3), 637–654. Retrieved September 4, 2023, from http://www.jstor.org/stable/1831029

Bollerslev, T. (1986) Generalized autoregressive conditional heteroskedasticity. *journal of Econometrics*, *31*, 307–327.

Brennan, M. J. (1979) The pricing of contingent claims in discrete time models. *The journal of finance*, *34*(1), 53–68.

Carr, P., and Sun, J. (2007) A new approach for option pricing under stochastic volatility. *Review of Derivatives Research*, *10*, 87–150.

Chorro, C., Guegan, D., and Ielpo, F. (2008) *Option Pricing under GARCH models with Generalized Hyperbolic distribution (II) : Data and Results* (Post-Print hal-00308687). HAL. https://ideas.repec.org/p/hal/journl/hal-00308687.html

Christoffersen, P., Elkamhi, R., Feunou, B., and Jacobs, K. (2010) Option valuation with conditional heteroskedasticity and nonnormality. *The Review of Financial Studies*, *23(5)*, 2139–2183.

Washburn, B., and Dik, M. (2021) *Derivation of black-scholes equation using itô's lemma*. https://doi.org/10.47086/pims.956201

Cox, J. C., Ross, S. A., and Rubinstein, M. (1979) Option pricing: A simplified approach. *Journal of Financial Economics*, *7*(3), 229–263. https://doi.org/https://doi.org/10.1016/0304-405X(79)90015-1

Duan, J.-C. (1995) The garch option pricing model. *Mathematical finance*, *5*(1), 13–32.

Engle, R. F. (1982) Autoregressive conditional heteroscedasticity with estimates of the variance of united kingdom inflation. *Econometrica*, *50*(4), 987–1007. Retrieved August 30, 2023, from http://www.jstor.org/stable/1912773

Engle, R. F., and Ng, V. K. (1993) Measuring and testing the impact of news on volatility. *The Journal of Finance*, *48*(5), 1749–1778. Retrieved August 31, 2023, from http://www.jstor.org/stable/2329066

Eric Jondeau, M. R., Ser-Huang Poon. (2010) *Financial modeling under non-gaussian distributions*. Springer London.

Heston, S. L. (1993) A closed-form solution for options with stochastic volatility with applications to bond and currency options. *The review of financial studies*, *6*(2), 327–343.

Heston, S. L., and Nandi, S. (2000) A closed-form garch option valuation model. *The Review of Financial Studies*, *13*(3), 585–625. Retrieved September 26, 2023, from http://www.jstor.org/stable/2645997

Hull, J., and White, A. (1987) The pricing of options on assets with stochastic volatilities. *The journal of finance*, *42*(2), 281–300.

Hull, J. C. (2012) *Options, futures, and other derivatives*. Pearson.

Jaeckel, P. (2002) *Monte carlo methods in finance*. WILEY.

J.P.Morgan/Reuters. (1996) *Technical document* (tech. rep.). RiskMetrics.

Longstaff, F., and Schwartz, E. (2001) Valuing american options by simulation: A simple least-squares approach. *Review of Financial Studies*, *14*, 113–47. https://doi.org/10.1093/rfs/14.1.113

Merton, R. C. (1973) Theory of rational option pricing. *The Bell Journal of Economics and Management Science*, *4*(1), 141–183. Retrieved September 4, 2023, from http://www.jstor.org/stable/3003143

Merton, R. C. (1976) Option pricing when underlying stock returns are discontinuous. *Journal of financial economics*, *3*(1-2), 125–144.

Natenberg, S. (2014) *Option volatility and pricing: Advanced trading strategies and techniques, 2nd edition*. McGraw Hill LLC. https://books.google.it/books?id=p9eoBAAAQBAJ

O'Neil, C., and Zumbach, G. (2009) *Using relative returns to accommodate fat tailed innovations in processes and option pricing.* (tech. rep.). RiskMetrics Group.

Pascucci, A. (2011) *Pde and martingale methods in option pricing*. Springer.

Rubinstein, M. (1976) The valuation of uncertain income streams and the pricing of options. *The Bell Journal of Economics*, 407–425.

Sinclair, E. (2010) *Option trading: Pricing and volatility strategies and techniques* (Vol. 445). John Wiley & Sons.

Stein, E. M., and Stein, J. C. (1991) Stock price distributions with stochastic volatility: An analytic approach. *Review of Financial Studies*, *4*, 727–752. http://rfs.oxfordjournals.org/

Zumbach, G. (2002) Volatility processes and volatility forecast with long memory. *Quant. Finance*, *4*, 70–86.

Zumbach, G. (2006) *The riskmetrics 2006 methodology* (tech. rep.). RiskMetrics.

Zumbach, G. (2012) Option pricing and arch processes. *Finance Research Letters*, *9*, 144–156.

Zumbach, G., and Fernández, L. (2013) Option pricing with realistic arch processes. *Quantitative Finance*, *14:1*, 143–170.

Zumbach, G., Fernández, L., and Weber, C. (2014) Processes for stocks capturing their statistical properties from one day to one year. *Quant. Finance*, *14:5*, 849–861.

Zumbach, G. (2009) Time reversal invariance in finance. *Quantitative Finance*, *9*(5), 505–515.

Zumbach, G. (2013) *Discrete time series, processes, and applications in finance*. Berlin; Heidelberg: Springer.